Bioorganic Chemistry 89 (2019) 103020

Contents lists available at ScienceDirect

Bioorganic Chemistry

journal homepage: www.elsevier.com/locate/bioorg

Bridged bicyclic 2,3-dioxabicyclo[3.3.1]nonanes as antiplasmodial agents: Synthesis, structure-activity relationships and studies on their biomimetic reaction with Fe(II)

Sarah D'Alessandro[a,1], Gloria Alfano[b,1], Luisa Di Cerbo[b], Simone Brogi[b,2], Giulia Chemi[b], Nicola Relitti[b], Margherita Brindisi[c], Stefania Lamponi[b], Ettore Novellino[c], Giuseppe Campiani[b,*], Sandra Gemma[b,*], Nicoletta Basilico[a], Donatella Taramelli[d], Maria Camilla Baratto[b], Rebecca Pogni[b], Stefania Butini[b]

[a] Department of Biomedical, Surgical and Dental Sciences, University of Milan, Via Pascal 36, 20133 Milan, Italy
[b] Department of Biotechnology, Chemistry and Pharmacy (DoE 2018-2022), University of Siena, via Aldo Moro 2, 53100 Siena, Italy
[c] Department of Pharmacy (DoE 2018-2022), University of Naples Federico II, via D. Montesano 49, 80131 Naples, Italy
[d] Department of Pharmacological and Biomolecular Sciences, University of Milan, Via Pascal 36, 20133 Milan, Italy

ARTICLE INFO

Keywords:
Plasmodium falciparum
Synthetic endoperoxides
Antimalarials
Bioactivation reaction
C-centered radicals
Docking studies

ABSTRACT

Despite recent advancements in its control, malaria is still a deadly parasitic disease killing millions of people each year. Progresses in combating the infection have been made by using the so-called artemisinin combination therapies (ACTs). Natural and synthetic peroxides are an important class of antimalarials. Here we describe a new series of peroxides synthesized through a new elaboration of the scaffold of bicyclic-fused/bridged synthetic endoperoxides previously developed by us. These peroxides are produced by a straightforward synthetic protocol and are characterized by submicromolar potency when tested against both chloroquine-sensitive and chloroquine-resistant *Plasmodium falciparum* strains. To investigate their mode of action, the biomimetic reaction of the representative compound **6w** with Fe(II) was studied by EPR and the reaction products were characterized by NMR. Rationalization of the observed structure-activity relationship studies was performed by molecular docking. Taken together, our data robustly support the hypothesized mode of activation of peroxides **6a-cc** and led to the definition of the key structural requirements responsible for the antiplasmodial potency. These data will pave the way in future to the rational design of novel optimized antimalarials suitable for *in vivo* investigation.

1. Introduction

The decline of malaria burden observed in the last years in malaria-endemic countries is due to a combination of several factors, including better diagnosis, extended use of artemisinin-based combination therapy (ACT), improved drug accessibility, wide distribution of insecticide-treated bed nets, and indoor residual spray measures [1]. Despite these recent progresses, malaria is still a deadly disease killing millions of people each year and resistance or decreased susceptibility to artemisinins has been observed in some regions [2,3]. Due to the importance of dihydroartemisin (DHA, **1**, Fig. 1) and semisynthetic derivatives, intense research efforts have been dedicated to the development of synthetic peroxides. Artefenomel (**2**) and arterolane (**3**) are two representative synthetic endoperoxides, undergoing clinical investigation and introduced in therapy, respectively [4,5]. Synthetic peroxides are not only a more economical alternative to artemisinins, but are also suitable for pharmacokinetic optimization. In this regard, improvement of pharmacokinetic properties of endoperoxides, and in particular an increase in their half-life compared to artemisinin has recently emerged as a critical factor that could improve efficacy against mutant K13 parasites showing decreased susceptibility or resistance to artemisinins [6–8]. The mode of action of artemisinins and related synthetic peroxides is still debated and not completely clarified. One of the hypothesis regarding their mode of action suggests that organic

* Corresponding authors at: Department of Biotechnology, Chemistry and Pharmacy, Siena, Italy.
E-mail addresses: campiani@unisi.it (G. Campiani), gemma@unisi.it (S. Gemma).
[1] These authors equally contributed to the present work.
[2] Current address: Department of Pharmacy, University of Pisa, via Bonanno 6, 56126 Pisa, Italy.

https://doi.org/10.1016/j.bioorg.2019.103020
Received 13 March 2019; Received in revised form 15 May 2019; Accepted 28 May 2019
Available online 31 May 2019
0045-2068/

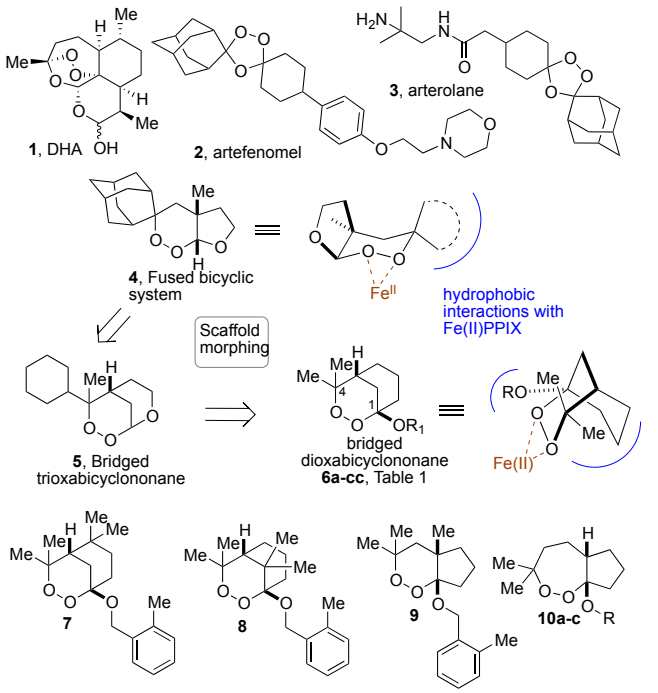

Fig. 1. Structure of reference (**1–5**) and newly designed (**6–10**) compounds. Bold and dashed lines indicate relative configuration of each carbon forming the bridge. Bridged bicyclic derivatives are obtained as racemic mixtures.

peroxides, endowed with specific structural features, react with Fe(II)-heme, present as a by-product of the hemoglobin metabolism inside the parasite food vacuole. Based on this hypothesis, the activity of peroxides is related to two critical events, first the interaction of the peroxide bond with Fe(II)-heme and, second, the reductive cleavage of the peroxide system with the formation of an O-centered radical. The subsequent evolution of the latter to a C-centered radical results in damage of proteins and membranes of the parasite [9–12]. Despite several studies point to Fe(II)-catalyzed activation of artemisinin and peroxide-containing compounds to form transient toxic species, there is no consensus about the actual Fe(II)-source required for bioactivation or the actual toxic species responsible for parasite killing [13–17]. Moreover, it has also been suggested that peroxide-containing compounds are able to overwhelm redox homeostasis in the parasite by inducing rapid oxidation of flavin cofactors used by flavoenzymes for maintaining reduced glutathione levels [18,19].

Since several years, we have been engaged in the total synthesis of dihydroplakortin, a naturally occurring endoperoxide with antimalarial activity [20]. Moreover the design and synthesis of novel synthetic endoperoxides characterized by diverse bicyclic scaffolds have also been carried out [20–24]. A first series of compounds characterized by a fused-bicyclic endoperoxide system typified by **4** was designed.

Based on the hypothesis that our compounds, analogously to what previously observed for plakortin and dihydroplakortin [25], could react with Fe(II)-heme and being activated to form a C-centered radical, we performed docking studies on the fused bicyclic structure of **4** and analogues, which suggested that the peroxide moiety is able to correctly interact with Fe(II)-heme and that the binding mode is stabilized by the formation of appropriate hydrophobic interactions between the C-skeleton of the peroxide and the protoporphyrin ring system [24]. To improve the activity of the compounds, we converted the fused-bicyclic core into a bridged-bicyclic scaffold (representative compound **5**, Fig. 1) which is also present in other natural endoperoxides such as Yangsozhou A [23]. Through a scaffold morphing approach, we present herein a further elaboration of the bridged bicyclic scaffold in which the oxygen adjacent to peroxide functionality was shifted from an endocyclic to an exocyclic position (compounds **6a-cc**, Fig. 1). This modification would result in a simplification of the overall synthetic strategy, while maintaining appropriate hydrophobic contacts of the carbon-skeleton with the protoporphyrin ring and making possible straightforward exploration of a wide variety of R1 substituents on the exocyclic oxygen for scaffold decoration and investigation of the structure-activity relationships. We also performed modification of the bicyclic scaffold through introduction of extra-methyl groups such as in compounds **7** and **8**. The introduction of dimethyl substituents on the scaffold was accomplished in order to validate the hypothesized binding mode of the compounds to free heme. Finally, we hybridized scaffolds **4** and **7** leading to the design and synthesis of compounds **9** and **10a-c**.

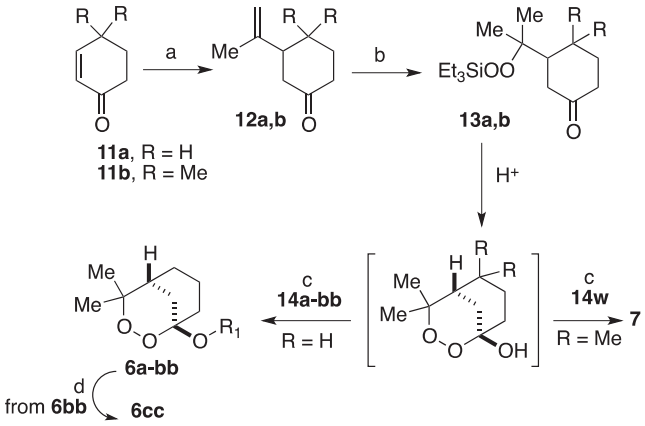

Scheme 1. a. CuI, isopropenylmagnesium bromide, dry THF, −78 °C, 3 h; b. Co(acac)$_2$, Et$_3$SiH, *t*-BuOOH, O$_2$, 1,2-DCE, 25 °C, 5 h; c. from **13a**: ROH **14a-bb**, *p*-TsOH, dry DCM, 25 °C, 1 h; d. from **13b**: **14w**, *p*-TsOH, dry DCM, 25 °C, 1 h; d. LiOH, H$_2$O/MeCN, 25 °C. Bold and dashed lines indicate relative configuration of each carbon forming the bridge. Bridged bicyclic derivatives are obtained as racemic mixtures.

2. Results and discussion

2.1. Chemistry

The title compounds **6a-bb** and **7** were synthesized by a straightforward 3-step procedure highlighted in Scheme 1.

Cyclohexenones **11a,b** were treated with propenylmagnesium bromide in the presence of CuI to afford the addition products **12a,b**. The Mukaiyama protocol was used to install the triethylsilylperoxide moiety. Due to the low steric hindrance of the propylene system, the Co-based catalyst Co(acac)$_2$ could be used instead of the more expensive Co(thd)$_2$ catalyst used in previous protocols [20,26]. Silylperoxides **13a,b** were then reacted under acidic conditions with the suitable alcohol to obtain peroxides **6a-bb** (Table 1) and **7** (Fig. 1). Due to ring constraints, only the regioisomer bearing each carbon forming the bridge *cis* to each other is formed. Accordingly, cyclized compounds are obtained as racemic mixtures. Compound **6cc** was obtained from compound **6bb** by a saponification reaction with LiOH. Non-commercially available alcohols necessary for the synthesis of final compounds listed in Table 1 have been prepared as described in the Supporting Information file (Table S1 and Schemes S1–5). Reaction yields of the last synthetic steps ranged from 10 to 55%.

To optimize the reaction yields for the deprotection/cyclization reaction, different conditions were explored as reported in Table 2. Different acidic catalysts were used: sulfonic acids or Lewis acids such as trimethylsilyl triflate, boron trifluoride, indium chloride or titanium chloride. We noted that Lewis acids generally provided the lowest yields, allowing the formation of final compound in trace amount or with yields lower than 20%, while better or comparable results were obtained by using sulfonic acids such as *p*TsOH or CSA.

Table 1
Antiplasmodial Activity of Compounds **6a-cc**, and of Reference Compounds DHA (**1**) and CQ.

Cpd	R	D10	W2	Cpd	R	D10	W2
		IC_{50} (μM)[a]				IC_{50} (μM)[a]	
6a		8.5	6.0	**6p**		2.4	1.4
6b		5.8	2.6	**6q**	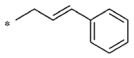	1.2	0.70
6c		3.4	1.5	**6r**	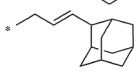	0.42	0.34
6d		1.7	1.1	**6 s**	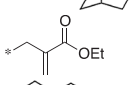	12.5	8.1
6e		0.80	0.49	**6 t**		0.80	0.43
6f	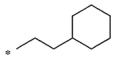	0.51	0.40	**6u**		1.31	0.622
6g	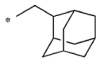	0.90	0.52	**6v**	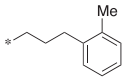	0.67	0.25
6h	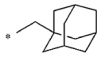	0.33	0.27	**6w**		0.74	0.63
6i	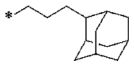	0.24	0.16	**6x**		0.89	0.44
6j	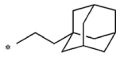	0.58	0.44	**6y**		3.0	1.5
6k		1.5	0.83	**6z**		0.98	0.70
6l		2.5	1.5	**6aa**		2.4	1.6
6m		1.6	0.92	**6bb**	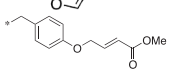	0.78	0.53
6n	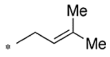	1.32	0.83	**6 cc**	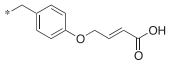	2.4	4.5
6o	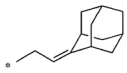	0.75	0.46		DHA, **1** CQ	0.0049 0.022	0.0046 0.409

[a] IC_{50} values are the mean of at least three experiments in duplicate; SD were within 30% of the mean.

Table 2
Yield optimization attempts for the reaction of **13** with **14w** to afford **6w**.

Entry	Acid	Solvent	Temperature	Time	Yield
1	*p*TsOH	DCM	25 °C	1 h	30%
2	*p*TsOH + MS 4 Å	DCM	25 °C	3 h	45%
3	CSA	DCM	25 °C	5 h	31%
4	CSA + MS 4 Å	DCM	25 °C	24 h	41%
5	TMSOTf	DCM	−78 °C	15 min	17%
6	$BF_3(OEt)_2$	DCM	25 °C	40 min	6%
7	PPTS	DCM	25 °C	20 h	Traces
8	$InCl_3$	MeCN	25 °C	24 h	Traces
9	$TiCl_4$	DCM	25 °C	2 h	5%

In both cases addition of 4 Å molecular sieves to remove the water formed during the reaction improved of the reaction yields. The main byproduct was the silylated alcohol. However, even when increasing the amount of alcohol, no better yields than those reported in Table 2, entries 2 and 4 were obtained.

The synthesis of peroxide **8** is reported in Scheme 2. Starting from cyclohexenone **11a**, methylation of the olefin was achieved through a two-step protocol. Firstly, α-iodination of cyclohexanone **11a** to **15** was accomplished using I_2 in the presence of K_2CO_3 and *N*,*N*-dimethylaminopyridine (DMAP). In the next step, alkenylation of the methylmagnesium bromide was performed in the presence of Fe(III) catalyst. Normant alkylcuprate addition on **16** was followed by regioselective α-alkylation of the resulting cyclohexanone to afford **17**. This latter intermediate was finally submitted to the hydroperoxysilylation-cyclization protocol to afford the final compound **8**.

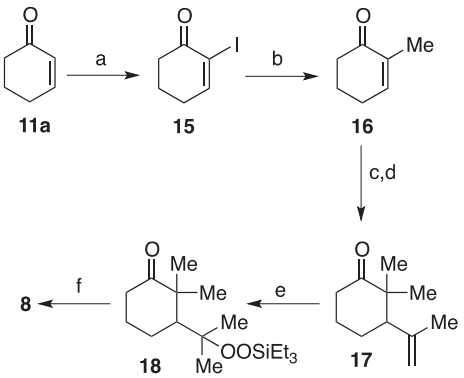

Scheme 2. a. I_2, K_2CO_3, DMAP, THF, H_2O, 0–25 °C, 3 h; b. $Fe(acac)_3$, MeMgBr, NMP, THF, 0–25 °C, 1 h; c. CuI, isopropenylmagnesium bromide, THF, −78 °C, 2.5 h; d. NaH, MeI, THF, reflux, 4 h; e. $Co(acac)_2$, Et_3SiH, *t*-BuOOH, O_2, 1,2-DCE, 25 °C, 5 h; f. **14w**, *p*-TsOH, dry DCM, 25 °C, 1 h.

Scheme 3 describes the synthetic procedure used for the preparation of peroxides **9** and **10a-c**. The key intermediate for the synthesis of **9** is

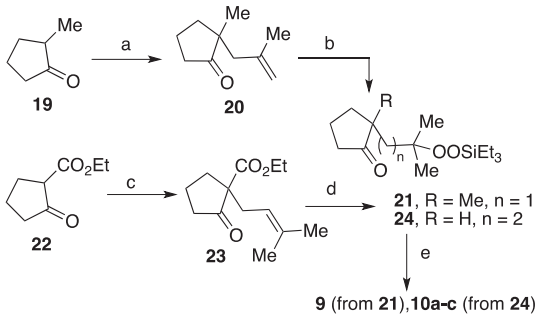

Scheme 3. a. 3-bromo-2-methylpropene, LDA, THF, −78 °C, 7.5 h; b. Co(acac)$_2$, Et_3SiH, *t*-BuOOH, O_2, 1,2-DCE, 25 °C, 5 h; c. 3-bromo-2-methylbut-2-ene; K_2CO_3, THF, 90 °C, 24 h; d. KOH, MeOH, reflux, 1 h; e. **14a** for **10a**, **14 h** for **10c** and **14w** (for **9** and **10b**), *p*-TsOH, dry DCM, 25 °C, 1 h.

the peroxide **21**, that was obtained by alkylation of α-methylketon **19** with 3-bromo-2-methylpropene in the presence of lithium diisopropylamide (LDA) and subsequent peroxysilylation of **20**. Intermediate **24**, necessary for the synthesis of **10a-c** was prepared starting from the β-ketoester **22** that was alkylated to **23**, and then decarboxylated and hydroperoxyslylated. Compounds **21** and **24** were cyclized to the corresponding final compounds following the usual protocol.

2.2. Antiplasmodial evaluation and structure-activity relationships

The *in vitro* antiplasmodial activity of the compounds was evaluated against a chloroquine-sensitive (CQ-S) D10 and a chloroquine-resistant (CQ-R) W2 strain of *P. falciparum*, as previously reported [24,27]. DHA was used as the control drug. The results are reported in Tables 1 and 3.

The simplest compounds of the series bear small alkyl chains as in **6a-c.** More branched R_1 side chains were introduced using alicyclic rings, spaced from the peroxyketal moiety by 1 to 3 carbon atoms (**6d-j**). Next, we introduced unsaturated groups with various spacers exploring terminal (**6l-m**), trisubstituted (**6n-p**) or disubstituted (**6q-r**) olefins. In compound **6s**, an activated Michael acceptor group was also introduced. Moreover, we sampled appended aromatic or heterocyclic substituents (**6t-aa**). Finally, an extended side chain bearing an ester or carboxylic acid group was also explored (**6bb,cc**). Overall, all peroxides here described presented an increased activity against the CQ-R over the CQ-S *P. falciparum* strain in line with the behavior of artemisinins and related synthetic endoperoxides. The most potent compounds were characterized by the presence of the adamantane moiety spaced by 1 to 3 carbon atoms (**6h-j,r**), with IC_{50} values lower than 0.24 μM. Also the compounds with an aromatic substituent showed interesting activities (**6t,v-x,z,bb**), with IC_{50} higher than those of compounds with the adamantane moiety but still lower than 1 μM. On the other hand, as outlined in Table 3, peroxides **7–9** and **10a-c** showed lower potency with respect to the original series.

To understand whether the antiplasmodial potency of our synthetic peroxides could be related to the lipophilicity of the substituent, the lipophilicity for compounds **6a-cc** was predicted *in silico* using ChemDraw with the "Chemical Properties" function, ACD/ChemSketch through the "Calculate logP" function, and QikProp calculation considering the QPlogPo/w parameter (Table S2 of the Supporting Information). Subsequently a correlation analysis between activity and lipophilicity was performed obtaining R^2 values clearly highlighting that potency of the peroxides was not merely dependent on lipophilicity for both CQ-S D10 and CQ-R W2 *P. falciparum* strains (Tables S2 and S3 of the Supporting Information).

2.3. Cytotoxicity evaluation

Cell viability on a selected set of analogues was evaluated *in vitro* against NIH3T3 cells after 24 h of contact, by Neutral Red Uptake (NRU) test. The cell line has been chosen because is a standard fibroblast cell line. Results of cytotoxicity tests are reported in Table 4. All compounds tested showed TC_{50} values in the high micromolar range well above antiplasmodial IC_{50} values.

Table 3
Antiplasmodial activity of compounds **7–9** and **10a-c.**

Cpd	R	D10	W2
		IC_{50} (μM)[a]	
7	-	> 16	8.9
8	–	8.2	3.4
9	–	> 30	> 30
10a		> 30	> 30
10b		> 30	> 30
10c	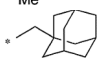	> 30	> 30
DHA, **1**		0.0049	0.0046
CQ		0.022	0.409

[a] IC_{50} values are the mean of at least three experiments in duplicate; SD were within 30% of the mean.

Table 4
TC_{50} values (μM) for a selected set of endoperoxides.

Cpd	TC_{50} (μM)[a]
6c	70
6d	37.5
6e	> 150
6f	140
6h	> 140
6k	95
6l	47.5
6m	28
6n	160
6x	140
6y	140
(DHA, 1)	> 140

[a] Data are expressed as mean of three experiments repeated in six replicates. SD are within 5% of the mean.

2.4. Study of the mode of activation of the peroxide moiety by Fe(II)

Several studies demonstrated that artemisinins and endoperoxides such as dioxanes, trioxanes and tetraoxanes could exert their mode of action by C-radical generation [11,12,28–30]. To examine if the generation of a C-radical is also possible for our bridged bicyclic dioxanes, we studied their reaction with Fe(II) salts using biomimetic reaction conditions [11,12,28–30].

2.4.1. Biomimetic reaction: analysis of the reaction products

The Fe(II) reaction of the representative compound **6w** was investigated in a biomimetic system consisting of a mixture of MeCN/H_2O in the presence of Fe(II) salts. We chose **6w** since it is endowed with submicromolar antimalarial activity and presents a tolyl moiety that would make easier to detect and structurally characterize the Fe(II)-mediated decomposition products. When peroxide **6w** was treated with 5 equivalents of $FeCl_2$ or $FeSO_4$, the formation of the same reaction product **25** was observed in almost quantitative yields after 2 h (Scheme 4). The ^{1}H- and COSY bidimensional- NMR experiments are reported in Fig. S1 of the Supporting Information.

2.4.2. EPR experiments

To detect the reaction species generated during Fe(II)-induced decomposition of **6w**, EPR experiments were performed. Low temperature

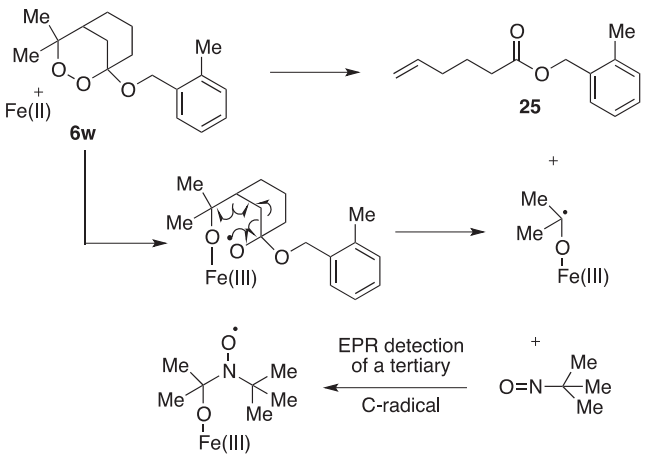

Scheme 4. Hypothesized reaction mechanism.

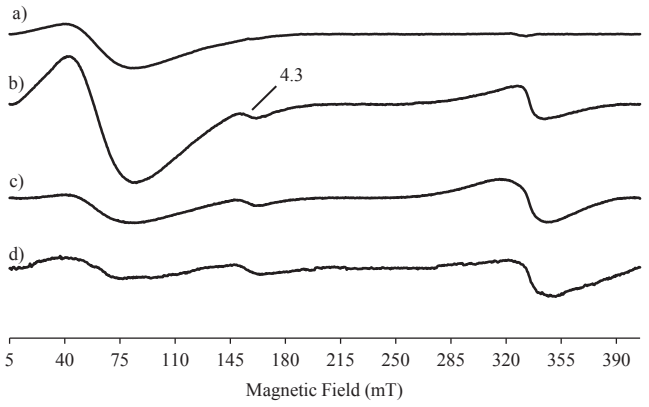

Fig. 2. CW X-band EPR spectra of: (a) Fe(II) salts in MeCN/H_2O mixture, (b) the reaction after 2 h of incubation, (c) the reaction after 4 h of incubation and d) the reaction after 36 h of incubation. Experimental conditions: ν = 9.388 GHz, 5mW microwave power, 1 mT for (a) and 0.2 mT for (b–d) modulation amplitude, T = 8 K.

X-band EPR spectra of the reaction mixture recorded at different reaction times are reported in Fig. 2. The first acquisition time is 2 h after the reaction starts (Fig. 2b) and, in agreement with the above-described reaction time, Fe(III) species with the signal at g = 4.3 due to the orthorhombic contribution, are formed and survived after 4 h and 36 h of reaction time (Fig. 2c and d). In Fig. 2a, the EPR spectrum of the Fe(II) salts in the MeCN/H_2O solvent is reported as a control.

Subsequently, peroxide **6w** was combined with $FeSO_4$ in the presence of the 2-methyl-2-nitrosopropane (MNP) C-radical spin trap in order to detect the radical species formed in concert with the Fe(III) formation. In Fig. 3, the EPR spectra at room temperature of the biomimetic reaction mixture (**6w** + Fe(II) + MNP in MeCN/H_2O) have been reported at different acquisition times. The spectra show that a C-radical species is trapped by the MNP with g = 2.0064 ± 0.0001 and a nitrogen coupling constant A_N = 1.5 ± 0.1 mT; the adduct lasts for 2 h. Thus the radical is a C tertiary radical as shown by the reaction mechanism proposed in Scheme 4 [31].

To exclude the presence of artifacts, MNP was reacted with Fe(II) and peroxide separately in the absence of **6w** and no EPR signal was detected (Fig. S2 of the Supporting Information).

Given together, these data suggest that the formation of olefin **25** can be explained assuming the reductive cleavage of the peroxide bond with the formation of an intermediate radical at O1. Following a β-scission mechanism [32,33], and a rearrangement of electrons, a terminal double bond is formed along with a radical at C4.

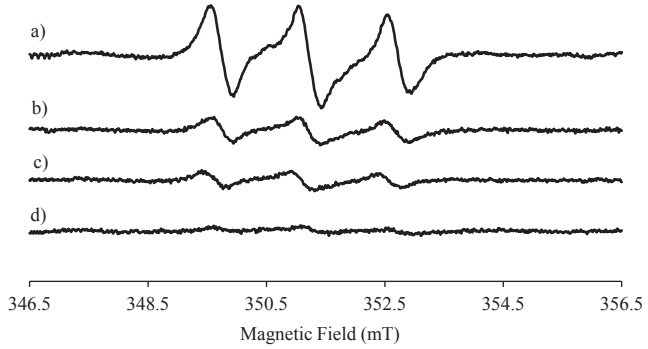

Fig. 3. X-band EPR spectra of the reaction in presence of the spin trap MNP at different reaction times: (a) t = 2 h, (b) t = 3 h, (c) t = 4 h and (d) t = 18 h. Experimental conditions: ν = 9.86 GHz, 5 mW microwave power, 0.1 mT modulation amplitude, T = 298 K.

2.5. Molecular docking

The above results prompted us to hypothesize that the difference in antiplasmodial potency of our peroxides could be related to a different ability of the compounds to interact with Fe(II)-heme. To verify this hypothesis, we investigated in depth the interaction of peroxides with Fe(II)-heme by performing computational studies based on molecular docking and relative ligand binding energies estimation. In particular, we analyzed the interaction of the peroxide moiety of compounds **6a–cc** with Fe(II)-heme by molecular docking studies employing Glide software, estimated the relative ligand binding energies by employing Prime software, and performed *ab initio* calculations employing Jaguar software. The protocol was used as previously reported [24]. Full details of our calculation are shown in Table S4. We observed a nice correlation between the distance of the peroxide oxygen atoms from the Fe(II) center of heme and the ligand binding energies with the antiplasmodial potency. The hydrophobic interaction established by the R_1 substituents and the protoporphyrine ring system can be visualized in Fig. S3.

Docking of one of the most active compounds (**6i**, IC_{50} 0.24 μM against D10 and 0.16 μM against W2) is reported in Fig. 4A. For this compound a strong metal coordination bond was found between oxygen atoms and Fe(II), since the O1-Fe and O2-Fe distances were 2.24 Å and 2.34 Å, respectively, and a ΔG_{bind} of −42.38 kcal/mol. The adamantyl group is able to stabilize the peroxide-Fe(II) coordination bond by forming hydrophobic interactions with the protoporphyrin ring (Fig. S3). Compound **6w** (Fig. 4B) is slightly less potent than **6i** (IC_{50} 0.74 μM against D10 and 0.63 μM against W2), in agreement with the less negative ΔG_{bind} of −40.05 kcal/mol, although its peroxide bond was still able to coordinate Fe(II) (distances O1-Fe and O2-Fe of 2.39 Å and 2.34 Å, respectively). The significant drop of antiplasmodial potency found for **6s** (Fig. 4C, IC_{50} 12.5 μM against D10 and 8.1 μM against W2) can be explained by considering the increased distances between O1-Fe and O2-Fe (3.10 Å and 3.00 Å, respectively) paralleled by a ΔG_{bind} value of −24.26 kcal/mol. As can be observed in the potential bioactive conformation of **6s** (Fig. 4C) the R_1 substituent does not correctly interact with the protoporphyrin ring establishing less hydrophobic contacts with it (Fig. S3).

3. Conclusions

Here we presented a novel class of endoperoxide antimalarials characterized by a bridged-bicyclic scaffold. A straightforward 3-steps protocol for the synthesis of these compounds was used that allowed the development of a significant number of analogues bearing functionalization at R_1. Several compounds showed submicromolar antimalarial potency. Chemical and EPR studies under biomimetic conditions are consistent with a mode of activation of the peroxide system by Fe(II)

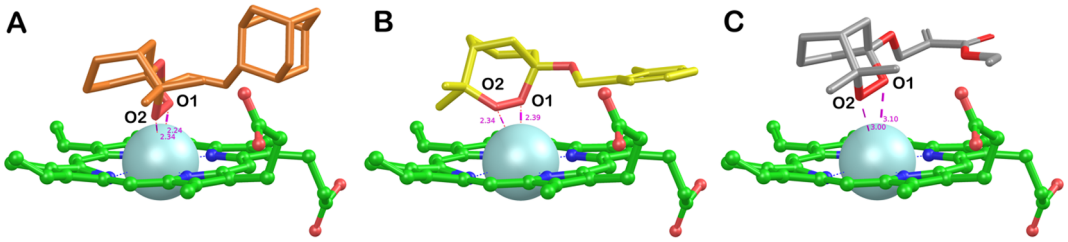

Fig. 4. Docked poses of compounds: **6i** (orange sticks in panel A), **6w** (yellow sticks in panel B) and **6s** (grey sticks in panel C) in complex with heme (green balls and sticks), charged iron was coloured cyan and represented by the CPK model. The potential ligand–metal coordination bonds are reported as red dotted lines while the distances are reported in magenta dotted lines. The picture was generated by Maestro.

leading to the formation of a C-centered radical intermediate. The observed differences in antiplasmodial potency were rationalized by *in silico* docking studies. Accordingly, we were able to relate the potency of the compounds with the distances of endoperoxide oxygen atoms from the Fe(II)-heme center and the relative ligand binding energies. The role of the side chain R_1 is the stabilization of the O-O——Fe(II) coordination bond by forming specific interactions with the protoporphyrin ring. The study of the mode of action of the bridged-bicyclic peroxides and the comprehension of the key determinant for their appropriate interaction with Fe(II)-heme suggest that their physicochemical and ADME properties, could be modulated in the future by rational modifications at the R_1 substituent.

4. Experimental section

4.1. Chemistry

Starting materials and solvents were purchased from commercial suppliers and used without further purification. Reaction progress was monitored by TLC using silica gel 60 F254 (0.040–0.063 mm) with detection by UV. Silica gel 60 (0.040–0.063 mm) was used for column chromatography. Yields refer to purified materials and are not optimized. ^{1}H NMR and ^{13}C NMR spectra were recorded on a Varian 300 MHz or a Bruker 400 MHz spectrometer using the residual signal of the deuterated solvent as internal standard. Splitting patterns are described as singlet (s), doublet (d), triplet (t), quartet (q), and broad (br); chemical shifts (δ) are given in ppm and coupling constants (*J*) in hertz (Hz). Mass spectra were recorded utilizing electrospray ionization (ESI). All moisture-sensitive reactions were performed under argon atmosphere using oven-dried glassware and anhydrous solvents. R* and S* indicate relative configuration at each carbon forming the bridge.

4.1.1. 3-(1-Propen-2-yl)cyclohexanone (12a)

To a −78 °C solution of isopropenylmagnesium bromide (0.5 M in THF, 6.66 mL, 3.33 mmol) in dry THF (10.0 mL) CuI (634.17 mg, 3.33 mmol) was added and the mixture was stirred for 1.5 h. 2-Cyclohexenone **11a** (200 mg, 2.08 mmol) was added and the resulting solution was stirred at −78 °C for another 1.5 h. A saturated solution of NH_4Cl (10.0 mL) was added dropwise and the mixture was allowed to cool to room temperature in 15 min. The blue residue was filtered through Celite™ and the solvent was removed in vacuo. Thereafter, the aqueous phase was extracted with DCM (3 × 10 mL) and the organic layer was dried over anhydrous Na_2SO_4, filtered and concentrated. The crude material was purified by flash chromatography (1:100 ethyl acetate/petroleum ether). Compound **12a** was obtained as pale volatile yellow oil (50% yield); ^{1}H NMR (300 MHz, $CDCl_3$) δ 4.77 (s, 1H), 4.72 (s, 1H), 2.48–2.15 (m, 5H), 2.15–1.99 (m, 1H), 1.99–1.84 (m, 1H), 1.73 (s, 3H), 1.71–1.49 (m, 2H); ^{13}C NMR (75 MHz, $CDCl_3$) δ 211.8, 147.7, 110.3, 46.9, 45.9, 41.5, 30.2, 25.4, 20.8.

4.1.2. 4,4-Dimethyl-3-(1-propen-2-yl)cyclohexanone (12b)

Starting from **11b**, the title compound was prepared following the procedure described for **12a** (11% yield); ^{1}H NMR (300 MHz, $CDCl_3$) 4.93–4.86 (m, 1H), 4.67–4.61 (m, 1H), 2.59–2.34 (m, 2H), 2.32–2.13 (m, 3H), 1.82–1.50 (m, 5H), 1.05 (s, 3H), 0.99 (s, 3H); ^{13}C NMR (75 MHz, $CDCl_3$) δ 212.0, 145.3, 113.7, 53.4, 43.4, 40.8, 38.1, 33.4, 29.5, 23.3, 20.6.

4.1.3. 3-(2-((Triethylsilyl)peroxy)propan-2-yl)cyclohexanone (13a)

To a stirred solution of **12a** (174 mg, 1.26 mmol) and $Co(acac)_2$ (0.324 g, 1.26 mmol) in dry 1,2-DCE (5.0 mL), under nitrogen atmosphere, triethylsilane (0.293 gg, 2.52 mmol) was added. Afterwards the atmosphere was saturated with oxygen and a drop of tert-butylhydroperoxide (5.0 M in nonane) was added. The resulting green mixture was stirred at 25 °C for 4 h, until consumption of the starting material. Thereafter the solvent was evaporated, and the resulting residue was purified by flash chromatography on silica gel (1:15 ethyl acetate/*n*-hexane) to afford **13a** as a colorless oil (90% yield); ^{1}H NMR (300 MHz, $CDCl_3$) δ 2.49–1.80 (m, 6H), 1.66–1.22 (m, 3H), 1.14 (d, J = 10.9 Hz, 6H), 1.00–0.84 (m, 9H), 0.69–0.48 (m, 6H); ESI-MS *m/z* 287 $[M+H]^+$, 309 $[M+Na]^+$.

4.1.4. 4,4-Dimethyl-3-(2-((triethylsilyl)peroxy)propan-2-yl) cyclohexanone (13b)

Starting from **12b**, the title compound was prepared following the procedure described for **13a**. The title compound was not isolated but was immediately used in the next reaction.

4.1.5. General procedure for the synthesis of 1-alkyl-4,4-dimethyl-2,3-dioxabicyclo[3.3.1]nonanes (6a-bb)

To a solution of compound **13a** (20 mg, 0.07 mmol) and the appropriate alcohol **14a-bb** (0.07 mmol) in dry DCM (3.0 mL), *p*-toluensulfonic acid (13 mg, 0.07 mmol) was added. The mixture was stirred for 1–6 h at 25 °C, then quenched with a saturated solution of $NaHCO_3$ and the aqueous phase was extracted with DCM (3 × 3.0 mL). The organic extracts were dried over anhydrous Na_2SO_4, filtered and concentrated. The title compounds were isolated as pure compounds by flash chromatography on silica gel.

4.1.6. (±)-(1R*,5S*)-1-Methoxy-4,4-dimethyl-2,3-dioxabicyclo[3.3.1] nonane (6a)

1:10 Ethyl acetate/ *n*-hexane; 55% yield; ^{1}H NMR (300 MHz, $CDCl_3$) 3.38 (s, 3H), 2.29–2.18 (m, 1H), 2.13–1.72 (m, 3H), 1.69–1.52 (m, 2H), 1.52–1.38 (m, 3H), 1.34 (s, 3H), 1.20 (s, 3H); ^{13}C NMR (75 MHz, $CDCl_3$) δ 104.0, 82.1, 49.3, 39.7, 32.2, 32.0, 25.9 (2C), 22.3, 21.3; ESI-MS *m/z* 209 $[M+Na]^+$.

4.1.7. (±)-(1R*,5S*)-1-Isopropoxy-4,4-dimethyl-2,3-dioxabicyclo [3.3.1]nonane (6b)

1:20 Ethyl acetate/petroleum ether; 30% yield; ^{1}H NMR (300 MHz, $CDCl_3$) δ 4.26–4.18 (m, 1H), 2.24–2.18 (m, 1H), 2.07–1.90 (m, 3H), 1.80–1.76 (m, 1H), 1.63–1.36 (m, 4H), 1.32 (s, 3H), 1.21 (s, 3H), 1.20–1.18 (m, 6H); ^{13}C NMR (75 MHz, $CDCl_3$) δ 104.1, 81.9, 64.6, 39.7, 33.8, 33.3, 26.0, 25.9, 24.9, 24.7, 22.4, 21.5; ESI-MS *m/z* 236 $[M+Na]^+$, 253 $[M+K]^+$.

4.1.8. (±)-(1R,5S*)-1-Isobutoxy-4,4-dimethyl-2,3-dioxabicyclo[3.3.1] nonane (**6c**)*

1:20 Ethyl acetate/petroleum ether; 30% yield; ^{1}H NMR (300 MHz, $CDCl_3$) δ 3.46–3.35 (m, 2H), 2.28–2.22 (m, 1H), 2.07–1.84 (m, 3H), 1.81–1.75 (m, 2H), 1.63–1.57 (m, 2H), 1.52–1.39 (m, 2H), 1.33 (s, 3H), 1.20 (s, 3H), 0.90 (d, J = 6.9 Hz, 6H); ^{13}C NMR (75 MHz, $CDCl_3$) δ 103.8, 82.0, 70.0, 68.3, 39.7, 33.1, 32.4, 29.0, 26.0, 22.3, 21.4, 19.6, 19.1; ESI-MS *m/z* 229 $[M+H]^+$, 251 $[M+Na]^+$, 267 $[M+K]^+$.

4.1.9. (±)-(1R,5S*)-1-(Cyclopentylmethoxy)-4,4-dimethyl-2,3-dioxabicyclo[3.3.1]nonane (**6d**)*

1:100 Ethyl acetate/petroleum ether, 11% yield; ^{1}H NMR (300 MHz, $CDCl_3$) δ 3.47–3.37 (m, 2H), 2.29–2.20 (m, 1H), 2.17–1.87 (m, 5H), 1.80–1.65 (m, 4H), 1.56–1.29 (m, 8H), 1.26 (s, 3H), 1.13 (s, 3H); ^{13}C NMR (75 MHz, $CDCl_3$) δ 103.5, 81.7, 65.8, 53.4, 39.7, 39.4, 32.9, 32.1, 29.6, 29.4, 25.8, 25.4, 25.3, 22.1, 21.1.

4.1.10. (±)-(1R,5S*)-1-(Cyclohexylmethoxy)-4,4-dimethyl-2,3-dioxabicyclo[3.3.1]nonane (**6e**)*

1:50 Ethyl acetate/petroleum ether; 11% yield); ^{1}H NMR (400 MHz, $CDCl_3$) δ 3.39–3.30 (m, 2H), 2.17 (d, 1H, J = 12.4 Hz), 1.99–1.85 (m, 3H), 1.73–1.30 (m, 12H), 1.26 (s, 3H), 1.23–1.04 (m, 7H); ^{13}C NMR (75 MHz, $CDCl_3$) 103.5, 81.7, 67.1, 53.4, 39.5, 38.3, 32.9, 32.1, 30.1, 30.0, 26.7, 25.9, 25.8, 25.7, 22.1, 21.14; ESI-MS *m/z* 269 $[M+H]^+$.

4.1.11. (±)-(1R,5S*)-1-(2-Cyclohexylethoxy)-4,4-dimethyl-2,3-dioxabicyclo[3.3.1]nonane (**6f**)*

1:50 Ethyl acetate/petroleum ether; 18% yield); ^{1}H NMR (400 MHz, $CDCl_3$) δ 3.62–3.52 (m, 2H), 2.19–2.16 (m, 2H), 1.99–1.86 (m, 3H), 1.64–1.52 (m, 7H), 1.39–1.35 (m, 8H), 1.25 (s, 3H), 1.20–108 (m, 5H); ESI-MS *m/z* 283 $[M+H]^+$, 305 $[M+Na]^+$.

4.1.12. (±)-(1R,5S*)-1-(Adamantan-2-ylmethoxy)-4,4-dimethyl-2,3-dioxabicyclo[3.3.1]nonane (**6g**)*

1:90 Diethyl ether/*n*- hexane; 21% yield; ^{1}H NMR (400 MHz, $CDCl_3$) δ 3.67–3.59 (m, 2H), 2.22–2.13 (m, 1H), 2.06–1.96 (m, 1H), 1.94–1.64 (m, 12H), 1.59–1.31 (m, 10*H*), 1.30–1.25 (m, 3H), 1.16–1.12 (m, 3H); ESI-MS *m/z* 343 $[M+Na]^+$.

4.1.13. (±)-(1R,5S*)-1-(Adamantan-1-ylmethoxy)-4,4-dimethyl-2,3-dioxabicyclo[3.3.1]nonane (**6h**)*

1:100 Diethyl ether/*n*-hexane; 45% yield; ^{1}H NMR (400 MHz, $CDCl_3$) δ 3.20–3.08 (m, 2H), 2.18 (d, 2H, J = 20,0 Hz), 2.06–1.80 (m, 6H), 1.73–1.52 (m, 10H), 1.44–1.32 (m, 6H), 1.30–1.25 (s, 3H), 1.16–1.12 (s, 3H); ESI-MS *m/z* 343 $[M+Na]^+$.

4.1.14. (±)-(1R,5S*)-1-(3-((1R,3S,5R,7R)-Adamantan-2-yl)propoxy)-4,4-dimethyl-2,3- dioxabicyclo[3.3.1]nonane (**6i**)*

1:50 Ethyl acetate/petroleum ether; 19% yield; ^{1}H NMR (300 MHz, $CDCl_3$) δ 3.71–3.52 (m, 2H), 2.30–2.19 (m, 1H), 2.10–1.74 (m, 16H), 1.74–1.38 (m, 11H), 1.32 (m, 3H), 1.21 (s, 3H); ^{13}C NMR (75 MHz, $CDCl_3$) δ 103.6, 81.8, 77.2, 62.0, 39.4, 39.3, 38.4, 32.8, 31.8, 31.6, 29.7, 28.9, 28.4, 28.3, 28.1, 25.7, 22.1, 21.1; ESI-MS *m/z* 349 $[M+H]^+$ 371 $[M+Na]^+$.

4.1.15. (±)-(1R,5S*)-4,4-Dimethyl-1-(2-propyn-1-yloxy)-2,3-dioxabicyclo[3.3.1]nonane (**6k**)*

1:20 Ethyl acetate/petroleum ether; 54% yield; ^{1}H NMR (300 MHz, $CDCl_3$) δ 4.33 (s, 1H), 2.41 (s,1H), 2.29–2.25 (m, 1H), 2.16–1.87 (m, 3H), 1.79–1.74 (m, 1H), 1.67–1.48 (m, 3H), 1.43–1.34 (m, 2H), 1.25 (s, 3H), 1.17 (s, 3H); ^{13}C NMR (75 MHz, $CDCl_3$) δ 104.7, 82.2, 80.9, 73.5, 49.9, 39.5, 32.7, 31.9, 25.7, 25.4, 21.9, 21.2.

4.1.16. (±)-(1R,5S*)-1-(Allyloxy)-4,4-dimethyl-2,3-dioxabicyclo [3.3.1]nonane (**6l**)*

1:20 Ethyl acetate/petroleum ether; 50% yield; ^{1}H NMR (300 MHz, $CDCl_3$) δ 6.00–5.87 (m, 1H), 5.27 (d, J = 17.4 Hz, 1H), 5.13 (d, J = 10.2 Hz, 1H), 4.19–4.12 (m, 2H), 2.28–2.23 (m, 1H), 2.09–1.89 (m, 3H), 1.81–1.75 (m, 1H), 1.66–1.36 (m, 4H), 1.34 (s, 3H), 1.19 (s, 3H); ^{13}C NMR (75 MHz, $CDCl_3$) δ 135.6, 116.6, 104.2, 82.2, 63.1, 39.7, 33.1, 32.4, 26.0, 25.9, 22.3, 21.4; ESI-MS *m/z*: 235 $[M+Na]^+$.

4.1.17. (±)-(1R,5S*)-1-(3-Buten-1-yloxy)-4,4-dimethyl-2,3-dioxabicyclo[3.3.1]nonane (**6m**)*

1:20 Ethyl acetate/petroleum ether; 52% yield; ^{1}H NMR (300 MHz, $CDCl_3$) δ 5.80–5.69 (m, 1H), 5.04–4.92 (m, 2H), 3.68–3.53 (m, 2H), 2.29–2.21 (m, 2H), 2.19–2.17 (m, 1H), 2.00–1.81 (m, 3H), 1.72–1.57 (m, 1H), 1.54–1.30 (m, 4H), 1.28 (s, 3H), 1.10 (s, 3H); ESI-MS *m/z* 249 $[M+Na]^+$.

4.1.18. (±)-(1R,5S*)-4,4-Dimethyl-1-((3-methylbut-2-en-1-yl)oxy)-2,3-dioxabicyclo[3.3.1]nonane (**6n**)*

1:90 Ethyl acetate/petroleum ether; 25% yield; ^{1}H NMR (300 MHz, $CDCl_3$) δ 5.36–5.31 (m, 1H), 4.17–4.15 (m, 2H), 2.33–2.25 (m, 1H), 2.07–1.88 (m, 3H), 1.72 (s, 3H), 1.67 (s, 3H), 1.64–1.37 (m, 5H), 1.33 (s, 3H), 1.20 (s, 3H).

4.1.19. (±)-(1R,5S*)-1-((Z)-2-(Adamantan-2-ylidene)ethoxy)-4,4-dimethyl-2,3-dioxabicyclo[3.3.1]nonane (**6o**)*

1:20 Diethyl ether/*n*-hexane; 10% yield; ^{1}H NMR (300 MHz, $CDCl_3$) δ 5.23 (t, 1H, J = 6.6 Hz) 4.25–4.15 (m, 2H), 2.83 (s, 1H), 2.37 (s, 1H), 2.28 (d, 1H, J = 12.6 Hz), 2.17–1.40 (m, 20H), 1.33 (s, 3H), 1.20 (s, 3H); ^{13}C NMR (75 MHz, $CDCl_3$) δ 151.6, 113.4, 103.8, 81.8, 57.4, 40.3, 39.6, 39.5, 38.8, 37.2, 33.0, 32.4, 32.2, 31.6, 30.9, 28.4, 25.7, 22.6, 22.1, 21.2; 14.1; ESI-MS *m/z*: 355 $[M+Na]^+$, 370.1 $[M+K]^+$.

4.1.20. (±)-(1R,5S*)-1-(1-Cyclohexen-1-ylmethoxy)-4,4-dimethyl-2,3-dioxabicyclo[3.3.1]nonane (**6p**)*

1:20 Diethyl ether/*n*-hexane; 11% yield); ^{1}H NMR (300 MHz, $CDCl_3$): δ 5.70 (s, 2H), 4.02 (t, 2H, J = 12.3 Hz), 2.27 (dq, 1H, J_1 = 2.4 Hz, J_2 = 9.9 Hz), 2.10–1.86 (m, 6H), 1.77 (d, 1H, J = 12.4 Hz), 1.67–1.36 (m, 8H), 1.34 (s, 3H), 1.19 (s, 3H); ^{13}C NMR (75 MHz, $CDCl_3$): 135.2, 124.3, 103.8, 81.8, 66.3, 53.4, 39.4, 32.9, 32.2, 25.9, 25.8, 25.0, 22.5, 22.4, 22.1, 21.2; ESI-MS *m/z* 289 $[M+Na]^+$.

4.1.21. (±)-(1R,5S*)-1-(Cinnamyloxy)-4,4-dimethyl-2,3-dioxabicyclo [3.3.1]nonane (**6q**)*

1:25 Ethyl acetate/petroleum ether; 10% yield; ^{1}H NMR (400 MHz, $CDCl_3$) δ 7.31–7.14 (m, 5H), 6.53 (d, J = 16.0 Hz, 1H), 6.27–6.20 (m, 1H), 4.33–4.24 (m, 2H), 2.25–2.22 (m, 2H), 2.04–1.85 (m, 3H), 1.74–1.71 (m, 2H), 1.59–1.33 (m, 2H), 1.29 (s, 3H), 1.14 (s, 3H); ESI-MS *m/z* 311 $[M+Na]^+$, 327 $[M+K]^+$.

4.1.22. (±)-(1R,5S*)-1-(((E)-3-((Adamantan-2-yl)allyl)oxy)-4,4-dimethyl-2,3-dioxabicyclo[3.3.1]nonane (**6r**)*

1:50 Diethyl ether/*n*-hexane; 25% yield; ^{1}H NMR (300 MHz, $CDCl_3$) δ 5.91 (dd, 1H, J_1 = 6.3 Hz, J_2 = 15.6 Hz), 5.62–5.53 (m, 1H), 4.25–4.12 (m, 2H), 2.40 (d, 1H, J = 5.4 Hz), 2.27 (d, 1H, J = 12.3 Hz), 2.10–1.69 (m, 15H), 1.66–1.36 (m, 7H), 1.33 (s, 3H), 1.20 (s, 3H); ^{13}C NMR (75 MHz, $CDCl_3$) δ 137.8, 126.0, 103.9, 81.8, 63.1, 46.7, 39.5, 38.7(3), 38.0, 33.0, 32.7, 32.3, 32.0 (3), 28.0, 27.8, 25.7, 22.1, 21.2; ESI-MS *m/z* 369 $[M+Na]^+$, 385 $[M+K]^+$.

4.1.23. (±)-(1R,5S*)-Ethyl-2-(((4,4-dimethyl-2,3-dioxabicyclo[3.3.1] nonan-1- yl)oxy)methyl)acrylate (**6s**)*

1:30 Diethyl ether/*n*-hexane; 13% yield; ^{1}H NMR (300 MHz, $CDCl_3$) δ 6.28 (s, 1H), 5.92 (s, 1H), 4.39 (t, 2H, J = 15.0 Hz), 4.21 (q, 2H, J = 7.2 Hz), 2.29 (d, 1H, J = 10.2 Hz), 2.10–1.92 (m, 3H), 1.80–1.64 (m, 2H), 1.62–1.37 (m, 4H),1.34 (s, 3H), 1.29 (t, 3H, J = 7.2 Hz), 1.19 (s, 3H); ^{13}C NMR (75 MHz, $CDCl_3$) δ 165.8, 137.9, 125.3, 104.2, 82.0, 60.6, 60.0, 39.5, 32.8, 32.1, 25.7, 25.6, 22.0, 21.2, 14.2; ESI-MS *m/z*: 307 $[M+Na]^+$, 323 $[M+K]^+$.

4.1.24. (±)-(1R,5S*)-4,4-Dimethyl-1-(benzyloxy)-2,3-dioxabicyclo [3.3.1]nonane (**6t**)*

1:90 Ethyl acetate/petroleum ether; 20% yield; ^{1}H NMR (300 MHz, $CDCl_3$) δ 7.41–7.27 (m, 5H), 4.72 (d, J = 3.5 Hz, 2H), 2.33 (m, 1H), 2.18–1.87 (m, 3H), 1.88–1.73 (m, 1H), 1.70–1.41 (m, 4H), 1.37 (s, 3H), 1.22 (s, 3H); ^{13}C NMR (75 MHz, $CDCl_3$) δ 139.1, 128.5 (2C), 127.9 (2C), 127.5, 104.4, 82.3, 64.0, 39.8, 33.3, 32.5, 26.0, 25.9, 22.3, 21.5; ESI-MS *m/z*: 285 $[M+Na]^+$, 301 $[M+K]^+$.

4.1.25. (±)-(1R,5S*)-4,4-Dimethyl-1-(phenethoxy)-2,3-dioxabicyclo [3.3.1]nonane (**6u**)*

1:90 Ethyl acetate/petroleum ether; 26% yield; ^{1}H NMR (300 MHz, $CDCl_3$) δ 7.35–7.09 (m, 5H), 3.92–3.72 (m, 2H), 2.89 (t, J = 7.6 Hz, 2H), 2.32–2.16 (m, 1H), 2.14–1.84 (m, 3H), 1.77 (m, 1H), 1.68–1.53 (m, 1H), 1.52–1.36 (m, 3H), 1.34 (s, 3H), 1.19 (s, 3H); ^{13}C NMR (75 MHz, $CDCl_3$) δ 139.1, 129.2 (2C), 128.5 (2C), 126.4, 104.0, 82.1, 62.8, 39.7 (2C), 37.1, 33.0, 32.3, 25.9, 22.3, 21.4; ESI-MS *m/z*: 299 $[M+Na]^+$, 315 $[M+K]^+$.

4.1.26. (±)-(1R,5S*)-4,4-Dimethyl-1-(3-(o-tolyl)propoxy)-2,3-dioxabicyclo[3.3.1]nonane (**6v**)*

1:50 Ethyl acetate/petroleum ether; 28% yield; ^{1}H NMR (300 MHz, $CDCl_3$) δ 7.17–7.04 (m, 4H), 3.76–3.58 (m, 2H), 2.66 (m, 2H) 2.28 (s, 3H), 2.12–1.72 (m, 5H), 1.69–1.38 (m, 6H), 1.33 (s, 3H), 1.20 (s, 3H); ^{13}C NMR (75 MHz, $CDCl_3$) δ 140.3, 136.0, 130.0, 128.8, 125.8, 103.6, 81.8, 65.8, 39.4, 32.8, 32.2, 30.6, 29.6, 25.7, 25.7, 22.1, 19.2.

4.1.27. (±)-(1R,5S*)-4,4-Dimethyl-1-((2-methylbenzyl)oxy)-2,3-dioxabicyclo[3.3.1]nonane (**6w**)*

1:25 Ethyl acetate/petroleum ether; 22% yield; ^{1}H NMR (300 MHz, $CDCl_3$) δ 7.37–7.33 (m, 1H), 7.18–7.12 (m, 3H), 4.64 (q, 2H, J = 11.7 Hz), 2.35 (s, 3H), 2.17–1.90 (m, 3H), 1.85–1.74 (m, 1H), 1.69–1.39 (m, 5H), 1.37 (s, 3H), 1.21 (s, 3H); ^{13}C NMR (75 MHz, $CDCl_3$) δ 136.7, 136.5, 130.1, 128.6, 127.6, 125.8, 104.2, 82.0, 62.0, 39.5, 32.9, 32.1, 25.8, 25.7, 22.1, 21.2, 18.8.

4.1.28. (±)-(1R,5S*)-1-((2-Ethylbenzyl)oxy)-4,4-dimethyl-2,3-dioxabicyclo[3.3.1]nonane (**6x**)*

1:50 Ethyl acetate/petroleum ether; 30% yield); ^{1}H NMR (300 MHz, $CDCl_3$) δ 7.36 (d, J = 7.2 Hz, 1H), 7.17 (m, 3H), 4.73 (q, 2H, J = 11.1 Hz), 2.71 (q, 2H, J = 7.5 Hz), 2.34 (d, 1H, J = 12.3 Hz), 2.16–1.90 (m, 3H), 1.80 (d, 1H, J = 14.4 Hz), 1.69–1.40 (m, 4H), 1.37 (s, 3H), 1.25–1.19 (m, 6H); ^{13}C NMR (75 MHz, $CDCl_3$) δ 142.4, 135.9, 129.1, 128.4, 127.8, 125.8, 104.1, 81.9, 61.6, 53.4, 39.5, 32.9, 32.1, 25.7, 25.2, 22.1, 21.2, 15.3.

4.1.29. (±)-(1R,5S*)-1-((2-Isopropylbenzyl)oxy)-4,4-dimethyl-2,3-dioxabicyclo[3.3.1]nonane (**6y**)*

1:20 Ethyl acetate/petroleum ether; 24% yield; ^{1}H NMR (300 MHz, $CDCl_3$) δ 7.35–7.28 (m, 3H), 7.17–7.11 (m, 1H), 4.75 (q, 2H, J = 11.1 Hz), 3.25 (q, 1H, J = 7.2 Hz), 2.36–2.32 (m, 1H), 2.10–1.40 (m, 8H), 1.37 (s, 3H), 1.24 (s, 3H), 1.22–1.16 (m, 6H).

4.1.30. (±)-(1R,5S*)-4,4-Dimethyl-1-(thiophen-2-ylmethoxy)-2,3-dioxabicyclo[3.3.1]nonane (**6z**)*

1:100 Ethyl acetate/petroleum ether), to afford the final compound **55** as a colorless oil (19% yield); ^{1}H NMR (400 MHz, $CDCl_3$) δ 7.18 (d, 1H, J = 5.2 Hz), 6.93 (s, 1H), 6.88 (t, 1H, J = 3.2 Hz), 4.86–4.78 (m, 2H), 2.26 (d, 1H, J = 11.4 Hz), 2.08–1.83 (m, 3H), 1.72 (d, 1H, J = 16 Hz), 1.61–1.33 (m, 4H), 1.31 (s, 3H), 1.14 (s, 3H); ^{13}C NMR (75 MHz, $CDCl_3$): δ 141.6, 126.3, 125.8, 125.3, 104.4, 81.7, 58.7, 39.5, 32.9, 31.6, 25.8, 25.6, 22.0, 21.2; ESI-MS *m/z*: 291 $[M+Na]^+$.

4.1.31. (±)-(1R,5S*)-1-(Furan-2-ylmethoxy)-4,4-dimethyl-2,3-dioxabicyclo[3.3.1]nonane (**6aa**)*

1:20 Eiethyl ether/*n*-hexane; 15% yield; ^{1}H NMR (300 MHz, $CDCl_3$) δ 7.39 (s, 1H), 6.32 (s, 2H), 4.71–4.62 (m, 2H), 2.36–2.25 (m, 1H), 2.11–1.90 (m, 3H), 1.78 (dd, 1H, J_1 = 2.4 Hz, J_2 = 14.7 Hz), 1.68–1.40 (m, 4H), 1.36 (s, 3H), 1.20 (s, 3H); ^{13}C NMR (75 MHz, $CDCl_3$) δ 152.1, 142.6, 110.3, 108.7, 104.3, 82.1, 56.2, 39.5, 32.8, 32.0, 25.8, 25.5, 22.0, 21.2; ESI-MS *m/z* 275 $[M+Na]^+$, 291 $[M+K]^+$.

4.1.32. (±)-(1R,5S*)-Methyl-4-(4-((((4,4-dimethyl-2,3-dioxabicyclo [3.3.1]nonan-1-yl)oxy)methyl) phenoxy)-2-butenoate (**6bb**)*

1:10 Ethyl acetate/*n*-hexane; 13% yield; ^{1}H NMR (300 MHz, $CDCl_3$) δ 7.29 (d, 2H, J = 8.4 Hz), 7.07 (dt, 1H, J_1 = 3.9 Hz, J_2 = 15.9 Hz), 6.85 (d, 2H, J = 8.4 Hz), 6.18 (d, 1H, J = 15.6 Hz), 4.68–4.64 (m, 4H), 3.75 (s, 3H), 2.31 (d, 1H, J = 12.3 Hz), 2.16–1.89 (m, 3H), 1.80 (d, 1H, J = 15.0 Hz), 1.68–1.41 (m, 4H), 1.36 (s, 3H), 1.21 (s, 3H); ^{13}C NMR (75 MHz, $CDCl_3$) δ 166.5, 157.4, 142.8, 131.7, 129.3(2), 121.5, 114.5(2), 104.1, 82.0, 66.4, 63.3, 51.6, 39.5, 33.1, 32.2, 25.7, 25.6, 22.1, 21.2.

4.1.33. (±)-(1R,5S*)-4-(4-(((4,4-Dimethyl-2,3-dioxabicyclo[3.3.1] nonan-1- yl)oxy)methyl) phenoxy)-2-butenoic acid (**6cc**)*

Compound **6bb** (10 mg, 0.03 mmol) was dissolved in MeCN (1.0 mL) and subsequently a solution of LiOH (1 mg, 0.03 mmol) in H_2O (500 µl) was added. The reaction was stirred at 25 °C for 12 h, then MeCN was evaporated and the aqueous residue (pH = 8) was extracted with EtOAc to eliminate impurities. Consequently, the aqueous phase was acidified by adding HCl 1 N at 0 °C dropwise and extracted with ethyl acetate (3 × 3 mL). Combined organics were dried over anhydrous Na_2SO_4, filtered and concentrated to give the desired compound **6cc** as an amorphous white solid (50% yield). ^{1}H NMR (300 MHz, CD_3OD) δ 7.26 (d, 2H, J = 8.4 Hz), 7.06 (dt, 1H, J_1 = 4.2 Hz, J_2 = 15.6 Hz), 6.91 (d, 2H, J = 8.4 Hz), 6.11 (d, 1H, J = 15.9 Hz), 4.72 (s, 2H), 4.61 (d, 2H, J = 3.6 Hz), 2.33 (d, 1H, J = 12.3 Hz), 2.11–1.85 (m, 3H), 1.82 (d, 1H, J = 14.4 Hz), 1.67–1.48 (m, 4H), 1.34 (s, 3H), 1.19 (s, 3H); ^{13}C NMR (75 MHz, CD_3OD) δ 168.1, 157.6, 143.2, 131.5, 129.1, 128.9(2), 121.4, 114.1(2), 104.1, 81.7, 66.1, 63.0, 39.4, 32.9, 31.5, 25.2, 24.6, 20.9.

*4.1.34. 4,4,6,6-Tetramethyl-1-((2-methylbenzyl)oxy)-2,3-dioxabicyclo [3.3.1]nonane (**7**)*

1:30 Ethyl acetate/petroleum ether; 31% yield; ^{1}H NMR (300 MHz, $CDCl_3$) δ 7.39–7.30 (m, 1H), 7.20–7.07 (m, 3H), 4.67 (q, 2H, J = 11.2 Hz), 2.35 (s, 3H), 2.31–2.19 (m, 1H), 1.98–1.82 (m, 3H), 1.80–1.64 (m, 1H), 1.56 (s, 3H), 1.42–1.21 (m, 2H), 1.15 (s, 3H), 1.13 (s, 3H), 1.08 (s, 3H); ^{13}C NMR (75 MHz, $CDCl_3$) δ 136.7, 136.6, 130.1, 128.7, 127.6, 125.8, 105.0, 84.5, 62.0, 51.6, 33.7, 33.5, 30.9, 30.4, 29.3, 28.3, 27.7, 25.9,18.8; ESI-MS *m/z* 327 $[M+Na]^+$.

*4.1.35. 2-iodocyclohex-2-enone (**15**)*

To a solution of **11a** (1000 mg, 10.40 mmol) in THF/H_2O (25:25 v/v) cooled at 0 °C, iodine (5.3 g, 20.80 mmol), K_2CO_3 (1.72 g, 12.5 mmol) and DMAP (254 mg, 2.08 mmol) were added. The reaction was stirred at 25 °C for 3 h, then it diluted with EtOAc. The organic layer was extracted, washed with a saturated solution of $Na_2S_2O_3$ and a 1 N solution HCl. The resulting solution was dried over anhydrous Na_2SO_4, filtered and concentrated. The residue was purified by flash chromatography on silica gel (1:5 ethyl acetate/petroleum ether) to afford the desired compound **15** as a pale-yellow solid (87% yield). ^{1}H NMR (300 MHz, $CDCl_3$) δ 7.76 (t, J = 4.4 Hz, 1H), 2.72–2.59 (m, 2H), 2.51–2.35 (m, 2H), 2.16–1.95 (m, 2H).

*4.1.36. 2-Methylcyclohex-2-enone (**16**)*

To a solution of **15** (2.46 g, 11.08 mmol) in dry THF (25 mL), Fe $(acac)_3$ (195 mg, 0.55 mmol) was added. Then the mixture was cooled to 0 °C and NMP (9.6 mL, 99.72 mmol) and MeMgBr (3 M in diethyl ether, 6.3 mL 18.84 mmol) were added dropwise. The color of the solution switched from orange to yellowish. The reaction was stirred at 25 °C for 1 h, then a 1 M solution of HCl was added and the mixture was extracted with diethyl ether (3 × 20 mL). The combined organics were

washed with a saturated solution of $NaHCO_3$, water and brine, dried over anhydrous Na_2SO_4, filtered and concentrated. The resulting residue was purified by flash chromatography on silica gel (1:10 ethyl acetate/pentane) to afford to give the desired compound **16** as volatile dark yellow oil (78% yield). ^{1}H NMR (300 MHz, $CDCl_3$) δ 6.74 (s, 1H), 2.46–2.37 (m, 2H), 2.37–2.26 (m, 2H), 2.07–1.90 (m, 2H), 1.77 (s, 3H); ^{13}C NMR (75 MHz, $CDCl_3$) δ 200.0, 145.6, 135.7, 38.3, 26.0, 23.3, 16.0.

4.1.37. 2,2-Dimethyl-3-(prop-1-en-2-yl)cyclohexanone (17)

Starting from **16**, 2-methyl-3-(propen-2-yl)cyclohexanone was prepared following the procedure described for **12a**. The crude material was purified by flash chromatography on silica gel (1:20 diethy ether/petroleum ether). Yield: 39%; ^{1}H NMR (300 MHz, $CDCl_3$) δ 4.89 (s, 1H), 4.65 (s, 1H), 2.70–1.89 (m, 5H), 1.88–1.60 (m, 6H), 0.97 (d, J = 7.1 Hz, 3H); ^{13}C NMR (75 MHz, $CDCl_3$) δ 215.1, 144.7, 111.7, 48.0, 47.0, 38.3, 24.7, 24.3, 22.5, 11.7; MS (IE) *m/z* 95 (100); 137; 123; 109; 95; 81; 67; 53. A solution of methyl-3-(propen-2-yl)cyclohexanone (90 mg, 0.60 mmol) in dry THF (1 mL) was added to a suspension of NaH (60% in mineral oil, 24 mg, 0.60 mmol) in dry THF (1 mL). The mixture was stirred at reflux for 1 h, then cooled down to 25 °C and MeI (170 mg, 1.20 mmol) was added. The reaction was stirred at 25 °C for 4 h then brine was added, and the mixture was extracted with diethyl ether (3 × 5 mL). The combined organics were washed with a saturated solution of $NaHCO_3$, water and brine, dried over anhydrous Na_2SO_4, filtered and concentrated. The resulting residue was purified by flash chromatography on silica gel (1:30 ethyl acetate/petroleum ether) to give the desired compound **17** as a colorless volatile oil (10% yield). ^{1}H NMR (300 MHz, $CDCl_3$) δ 4.94–4.90 (m, 1H), 4.68–4.65 (m, 1H), 2.61–2.46 (m, 1H), 2.37–2.23 (m, 1H), 2.16 (dd, $J1$ = 11.1 Hz, $J2$ = 3.6 Hz, 1H), 2.07–1.82 (m, 2H), 1.78–1.56 (m, 5H), 1.10 (s, 3H), 1.06 (s, 3H); MS (IE) *m/z* 166; 151; 123; 109; 95; 81; 67 (100).

4.1.38. 2,2-Dimethyl-3-(2-((triethylsilyl)peroxy)propan-2-yl) cyclohexanone (18)

Starting from **17**, the title compound was prepared following the procedure described for **13a**. The title compound was isolated as pure compounds by flash chromatography on silica gel (1:50 ethyl acetate/petroleum ether) to give the desired compound **18** as a colorless oil (33% yield). ^{1}H NMR (300 MHz, $CDCl_3$) δ 2.47–2.34 (m, 2H), 2.08–1.85 (m, 3H), 1.77–1.62 (m, 2H), 1.33–1.26 (m, 9H), 1.18 (s, 3H), 0.96 (t, J = 7.8 Hz, 9H), 0.71–0.58 (m, 6H); ESI-MS *m/z* 337 $[M+Na]^+$.

4.1.39. (±)-(1S*, 5R*)-4,4,9,9-Tetramethyl-1-((2-methylbenzyl)oxy)-2,3-dioxabicyclo[3.3.1]nonane (8)

Starting from **18**, the title compound was prepared following the general procedure described for compounds **6a-bb, 7**. The title compound was isolated as pure compounds by flash chromatography on silica gel (1:50 ethyl acetate/petroleum ether) to give the desired compound **5** as a colorless oil (20% yield). ^{1}H NMR (300 MHz, $CDCl_3$) δ 7.43–7.29 (m, 1H), 7.23–7.05 (m, 3H), 4.70 (d, J = 11.8 Hz, 1H), 4.50 (d, J = 11.8 Hz, 1H), 2.30 (s, 3H), 2.19–2.06 (m, 1H), 2.04–1.58 (m, 6H), 1.45 (s, 3H), 1.40 (s, 3H), 1.35 (s, 3H), 1.17 (s, 3H); ^{13}C NMR (75 MHz, $CDCl_3$) δ 137.2, 136.2, 129.8, 127.6, 127.1, 125.6, 107.0, 83.8, 61.3, 48.7, 39.0, 29.5, 27.2, 26.5, 26.4, 25.5, 21.7, 20.0, 18.8; ESI-MS *m/z* 327 $[M+Na]^+$.

4.1.40. 2-Methyl-2-(2-methylallyl)cyclopentanone (20)

A solution of DIPA (1.04 mL, 7.41 mmol) in dry THF (9 mL) was cooled at −78 °C and a 2.5 M solution of *n*-BuLi (2.69 mL, 6.74 mmol) in THF was added. The resulting mixture was stirred at the same temperature for 30 min, followed by the addition of **19** (825 mg, 8.41 mmol). The reaction was stirred at −78 °C for 3 h, and 3-bromo-2-methylpropene (1.7 mL, 16.82 mmol) was added and the mixture was allowed to reach 25 °C and stirred for 4 h. Thereafter, a saturated solution of NH_4Cl (10 mL) was added and the mixture was extracted with diethyl ether (3 × 10 mL). The combined organics were dried over anhydrous Na_2SO_4, filtered and concentrated. The resulting residue was purified by flash chromatography on silica gel (1:80 diethyl ether/petroleum ether) to give the desired compound **20** as a colorless oil (43% yield). ^{1}H NMR (300 MHz, $CDCl_3$) δ 4.83 (s, 1H), 4.68 (s, 1H), 2.33–2.24 (m, 1H), 2.24–2.09 (m, 3H), 2.05–1.78 (m, 4H), 1.67 (s, 3H), 0.99 (s, 3H). ^{13}C NMR (75 MHz, $CDCl_3$) δ 223.3, 142.2, 114.7, 48.3, 44.6, 37.4, 35.3, 24.2, 22.6, 18.6.

4.1.41. 2-Methyl-2-(2-methyl-2-((triethylsilyl)peroxy)propyl) cyclopentanone (21)

Starting from **20**, the title compound was prepared following the procedure described for **13a**. **21** was isolated by flash chromatography on silica gel (1:20 diethyl ether/petroleum ether) as a colorless oil (73% yield). ^{1}H NMR (300 MHz, $CDCl_3$) δ 2.37–2.12 (m, 3H), 2.01–1.86 (m, 2H), 1.84–1.77 (m, 1H), 1.73 (d, 1H, J = 15.2 Hz), 1.59 (s, 1H), 1.23 (s, 3H), 1.14 (s, 3H), 1.00 (s, 3H), 0.96 (t, 9H, J = 7.9 Hz), 0.65 (q, 6H, J = 7.9 Hz); ESI-MS *m/z* 323 $[M+Na]^+$.

4.1.42. 3,3,4a-Trimethyl-7a-((2-methylbenzyl)oxy)hexahydro-3H-cyclopenta[c][1,2]dioxine (9)

Starting from **21**, the title compound was prepared following the procedure described for **6a-bb,7**. The title compound purified by flash chromatography on silica gel (1:30 ethyl acetate/petroleum ether) to give the desired compound **9** as a colorless oil (7% yield). ^{1}H NMR (300 MHz, $CDCl_3$) δ 7.41 (m, 2H), 7.15 (m, 2H), 4.78 (d, 1H, J = 12.3 Hz), 4.40 (d, 1H, J = 12.3 Hz), 2.32 (s, 3H), 2.04 (m, 4H), 1.60 (m, 4H), 1.16 (s, 6H), 1.07 (s, 3H); ESI-MS *m/z* 313 $[M+Na]^+$.

4.1.43. Ethyl 1-(3-methylbut-2-en-1-yl)-2-oxocyclopentanecarboxylate (23)

To a solution of **22** (500 mg, 3.20 mmol) in dry THF (10 mL), K_2CO_3 (1.77 g, 12.8 mmol) was added. The mixture was stirred at 25 °C for 30 min, and 4-bromo-2-methyl-2-butene (2.59 g, 17.3 mmol) was added and the reaction was stirred at 90 °C for 24 h. The mixture was filtered through paper and a saturated solution of NH_4Cl (20 mL) was added, the mixture was extracted with DCM (3 × 10 mL). The combined organics were dried over anhydrous Na_2SO_4, filtered and concentrated. The resulting residue was purified by flash chromatography on silica gel (1:30 ethyl acetate/petroleum ether) to give the desired compound **23** as a yellow oil (70% yield). ^{1}H NMR (300 MHz, $CDCl_3$) δ 5.00 (t, 1H, J = 7.5 Hz), 4.15 (q, 2H, J = 7.1 Hz), 2.60 (dd, 1H, J_1 = 14.4 Hz, J_2 = 7.6 Hz), 2.34 (ddt, 4H, J_1 = 35.2 Hz, J_2 = 26.9 Hz, J_3 = 9.2 Hz), 2.03–1.82 (m, 3H), 1.69 (s, 3H), 1.61 (s, 3H), 1.24 (t, 3H, J = 7.1 Hz); ESI-MS *m/z* 247 $[M+Na]^+$.

4.1.44. 2-(3-Methyl-3-((triethylsilyl)peroxy)butyl)cyclopentan-1-one (24)

To a solution of **23** (449 mg, 2.00 mmol) in methanol (4 mL) a 4 M solution of KOH (1.72 mL) was added. The reaction was stirred at 90 °C for 1 h, then it was diluted with water (5 mL) and extracted with DCM (3 × 10 mL). The combined organics were dried over anhydrous Na_2SO_4, filtered and concentrated. The resulting residue was purified by flash chromatography on silica gel (1:20 ethyl acetate/petroleum ether) to give 2-(3-methylbut-3-en-1-yl)cyclopentanone as a yellow oil (47% yield). ^{1}H NMR (300 MHz, $CDCl_3$) δ 5.09 (d, 1H, J = 7.2 Hz), 2.46–2.24 (m, 2H), 2.05 (ddd, 6H, J_1 = 38.8 Hz, J_2 = 23.3 Hz, J_3 = 15.0 Hz), 1.76 (dd, 1H, J_1 = 18.3 Hz, J_2 = 8.2 Hz), 1.69 (s, 3H), 1.61 (s, 3H).

From this latter compound, following the procedure described to get compound **13a** the title compound was synthetized. **24** was isolated by flash chromatography on silica gel (1:40 ethyl acetate/petroleum ether) as a colorless oil (54% yield). ^{1}H NMR (300 MHz, $CDCl_3$) δ 2.25 (ddd, 2H, J_1 = 18.1 Hz, J_2 = 16.5 Hz, J_3 = 6.9 Hz), 2.09 (dd, 1H, J_1 = 17.9, J_2 = 9.2 Hz), 2.05–1.92 (m, 2H), 1.87–1.67 (m, 2H), 1.64–1.45 (m, 3H), 1.34–1.20 (m, 1H), 1.18 (s, 3H), 1.16 (s, 3H), 0.97 (t, 9H, J = 7.9 Hz), 0.65 (q, 6H, J = 7.9 Hz); ESI-MS *m/z* 324 $[M+Na]^+$.

4.1.45. 8a-Methoxy-3,3-dimethyloctahydrocyclopenta[c][1,2]dioxepine (10a)

Starting from **24** and **14a**, the title compound was prepared following the procedure described for **6a-bb,7**. **10a** was isolated by flash chromatography on silica gel (1:30 ethyl acetate/petroleum ether) as a colorless oil (71% yield). ^{1}H NMR (300 MHz, $CDCl_3$) δ 3.31 (s, 3H), 2.21–2.10 (m, 1H), 2.00–1.83 (m, 2H), 1.78–1.64 (m, 4H), 1.62–1.50 (m, 4H), 1.39 (s, 3H), 1.12 (s, 3H).

4.1.46. 3,3-Dimethyl-8a-((2-methylbenzyl)oxy)octahydrocyclopenta[c][1,2]dioxepine (10b)

Starting from **24** and **14w**, the title compound was prepared following the procedure described for **6a-bb,7**. **10b** was isolated by flash chromatography on silica gel (1:20 ethyl acetate/petroleum ether) as a colorless oil (7% yield). ^{1}H NMR (300 MHz, $CDCl_3$) δ 7.44 (m, 1H), 7.16 (m, 3H), 4.72 (d, 1H, J = 11.9 Hz), 4.45 (d, 1H, J = 11.9 Hz), 2.36 (s, 2H), 2.28 (m, 2H), 1.96 (m, 4H), 1.64 (m, 6H), 1.25 (s, 3H), 1.12 (s, 3H); ^{13}C NMR (75 MHz, $CDCl_3$) δ 137.0, 136.3, 129.9, 128.2, 125.7, 117.8, 82.4, 62.2, 49.1, 39.2, 31.9, 31.6, 29.7, 27.1, 26.5, 24.4, 22.7, 18.9; ESI-MS m/z 313 $[M+Na]^+$.

4.1.47. 8a-((Adamantan-1-yl)methoxy)-3,3-dimethyloctahydrocyclopenta[c][1,2]dioxepine (10c)

Starting from **24** and **14 h**, the title compound was prepared following the procedure described for **6a-bb,7**. **10c** was isolated by flash chromatography on silica gel (1:100 ethyl acetate/petroleum ether) as a colorless oil (18% yield). ^{1}H NMR (300 MHz, $CDCl_3$) δ 3.19 (d, J = 9.2 Hz, 1H), 2.91 (d, J = 9.2 Hz, 1H), 2.15 (d, J = 12.0 Hz, 2H), 1.90–1.75 (m, 2H), 1.66 (dt, 10*H*, J_1 = 11.4 Hz, J_2 = 6.6 Hz), 1.60–1.53 (m, 9H), 1.53–1.38 (m, 3H), 1.36 (s, 3H), 1.08 (s, 3H).

4.1.48. Biomimetic reaction: 2-methylbenzyl hex-5-enoate (25)

To a solution of **6w** (10 mg, 0.036 mmol) in a mixture of MeCN/water (4:1, 2 mL) a suspension of $FeCl_2{\cdot}4H_2O$ (36 mg, 0.18 mmol) in a mixture of MeCN/water (4:1, 2 mL) was added. The reaction was stirred into dark for 2 h. The mixture was extracted with ethyl acetate (3 × 5 mL) and the combined organic layers were dried over anhydrous Na_2SO_4, filtered and concentrated. The resulting residue was purified by flash chromatography on silica gel (1:50 ethyl acetate/petroleum ether) to give the desired compound **25** as a white solid (76% yield). ^{1}H NMR (300 MHz, $CDCl_3$) δ 7.39–7.10 (m, 4H), 5.87–5.63 (m, 1H), 5.11 (s, 2H), 5.07–4.90 (m, 2H), 2.45–2.25 (m, 5H), 2.18–1.96 (m, 2H), 1.83–1.63 (m, 2H); ^{13}C NMR (75 Hz, $CDCl_3$): δ 173.4, 137.6, 136.9, 133.9, 130.3, 129.2, 128.5, 126.0, 115.4, 64.5, 33.5, 33.0, 24.0, 18.8; ESI-MS m/z 241 $[M+Na]^+$.

4.2. EPR experiments

CW X-band (ν = 9 GHz) EPR measurements were carried out with an E580 Elexsys Series spectrometer (Bruker Biospin GmbH, Rheinstetten, Germany), Bruker ER 049X microwave bridge with a 4122SHQE/0208 cavity. For low temperature spectra an Oxford helium continuous flow cryostat (ESR 900, Oxford Instruments) was used. 3 × 4 mm I.D. × O.D. suprasil tubes were used for the EPR experiments.

Sample preparation: biomimetic reaction of **6w** with $FeSO_4$ were run as described in 4.1.40. For spin trap experiments, to a solution of **6w** (10 mg, 0.036 mmol) and MNP (0.36 mmol) in a mixture of MeCN/water (4:1, 2 mL), a suspension of $FeCl_2{\cdot}4H_2O$ (36 mg, 0.18 mmol) in a mixture of MeCN/water (4:1, 2 mL) was added. The reaction was stirred into dark and aliquots were taken up at regular interval times (2, 3, 4 and 18 h) for EPR measurements.

4.3. In vitro antiplasmodial evaluation

P. falciparum parasited were cultured according to the method of Trager and Jensen [34], with minor modifications [35]. CQ sensitive (D10) or CQ resistant (W2) strains were maintained at 5% hematocrit of human type A-positive red blood cells in RPMI 1640 medium (EuroClone; Celbio) containing 1% AlbuMAX II (lipid-rich bovine serum albumin), 24 mM sodium bicarbonate, 0.01% hypoxanthine, 20 mM HEPES, and 2 mM glutamine. All the cultures were maintained at 37 °C in a standard gas mixture consisting of 1% O_2, 5% CO_2, and 94% N_2.

Compounds were dissolved in dimethyl sulfoxide (DMSO) and then diluted with medium to achieve the required concentrations (final DMSO concentration < 1%, nontoxic to the parasites). Serial dilutions were made in a final volume of 100 µL/well in 96-well plates. Asexual parasite stages derived from asynchronous cultures with parasitemia of 1 to 1.5% were distributed into the plates (100 µL/well; final hematocrit, 1%) and incubated for 72 h at 37 °C. CQ and DHA were used as a reference control drugs. Parasite growth was determined by measuring the activity of the parasite lactate dehydrogenase (pLDH), according to a modified version of the spectrophotometric Makler's method [36]. Briefly, the drug-treated culture was resuspended, and 20 µL/well was transferred to a plate containing 100 µL of Malstat reagent (0.11% [vol/vol] Triton-100, 115.7 mM lithium L-lactate, 30.27 mM Tris, 0.62 mM 3-acetylpyridine adenine dinucleotide [APAD] [Sigma-Aldrich], adjusted to pH 9 with 1 M HCl) and 25 µL of PES/NBT (1.96 mM nitroblue tetrazolium chloride-0.24 mM phenazine ethosulfate). After few minutes incubation in the dark, absorbance was read (wavelength 650 nm) using a microplate reader, Synergy4 (BioTek). The antiplasmodial activity is expressed as the 50% inhibitory concentration (IC_{50}). Each IC_{50} value presented in Tables 1–3 is the mean and standard deviation of three independent experiments performed in duplicate.

4.4. Cytotoxicity

The *in vitro* acute toxicity of test compounds was evaluated using direct contact tests following the procedure proposed by ISO 10995-5 [37]. As the *in vitro* acute toxicity does not depend on the product's intended use, mouse fibroblasts NIH3T3 were used to test samples.

NIH3T3 were propagated in DMEM supplemented with 10% fetal calf serum, 1% L-glutamine-penicillin-streptomycin solution and 1% non-essential amino acid solution and incubated at 37 °C in a humidified atmosphere containing 5% CO_2. Once at confluence, cells were washed twice with 0.1 mol/L phosphate buffer saline, detached with trypsin-ethylenediaminetetraacetic acid solution and centrifuged at 1500 r.p.m. (rounds per minute) for 5 min. The pellet was then suspended in complete fresh medium (dilution 1:15) in order to have 1.5×10^4 cells/mL.

1 mL of cell suspension was then seeded in each well of a 24-well plate and incubated at 37 °C in an atmosphere of 5% CO_2. When cells reached 50% of confluence, the test compounds were added to each well. The tested concentrations of each samples ranged from 7 to 160 µM. All samples were set up in six replicates. Complete medium was used as a negative control. Cells were incubated in the test compounds for 24 h and then cell viability was evaluated through Neutral Red Uptake test (NRU).

4.4.1. Evaluation of NIH3T3 viability: NRU test

The following solutions were prepared in order to determine the percentage of viable cells after 24 h of contact with the test samples:

1. Neutral Red (NR) stock solution: 0.33 g NR dye powder in 100 mL sterile H_2O
2. NR medium: 1.0 mL NR stock solution + 99.0 routine culture medium pre-warmed to 37 °C
3. NR desorb solution: 1% glacial acetic acid solution + 50% ethanol + 49% H_2O

At the end of incubation, the routine culture medium was removed from each plate and the cells were carefully rinsed with 1 mL pre-warmed PBS 0.1 M. Plates were then gently blotted with paper towels.

1.0 mL NR medium was added to each dish and further incubated at 37 °C, 95% humidity, 5.0% CO_2 for 3 h. The cells were checked during incubation for NR crystal formation. After incubation, the NR medium was removed and the cells were carefully rinsed with 1 mL pre-warmed D-PBS 0.1 M. PBS was decanted and blotted from the dishes and exactly 1 mL NR desorb solution was added to each sample. Plates were placed on a shaker for 20–45 min to extract NR from the cells and form a homogeneous solution. During this step the samples were covered to protect them from light. Five minutes after removal from the shaker, absorbance was read at 540 nm with a UV/visible spectrophotometer (Lambda 25, Perkin Elmer).

4.5. Computational details

4.5.1. Fe(II)-heme and ligands preparation

The heme was firstly extracted from the Protein Data Bank (PDB) structure 1CTJ and prepared removing all the parts of the pdb crystal structure except for the porphyrin ring, and the Fe ion charged as +2 and prepared, as specified in the next paragraph, for acquiring appropriate starting complex for the subsequent computational analyses.

Compounds **6a-cc** were designed in Maestro Schrödinger environment and subsequently treated by means of LigPrep application [38], generating the most plausible ionization state at cellular pH value (7.4 ± 0.2). For retrieving the lower energy starting structures to use as input in molecular docking experiments, the prepared structures were analyzed by means of MacroModel [39]. The calculation was performed using OPLS-2005 as force field. The Generalized-Born/Surface-Area (GB/SA) model for simulating the solvent effects was used. No cutoff for non-bonded interactions was used. PRCG method was employed with 1000 maximum iterations and 0.001 gradient convergence threshold for performing the molecular energy minimizations. MCMM (Monte Carlo Multiple Minimum) was employed as torsional sampling method for the conformational searches, performing automatic setup with 21 kJ/mol (5.02 kcal/mol) in the energy window for saving structure and 0.5 Å was used as cutoff distance for redundant conformers [22].

4.5.2. Ab initio QM calculations

The endoperoxides and the heme structure were treated using a protocol already described [24]. The optimization was performed by Jaguar [40], using B3LYP hybrid density functional method in combination with the LACVP* basis set, which is composed of 6-31G* description for all light atoms and of LANL2DZ for metal center such as iron. LACVP basis set has been successfully used in calculation on metalloporphyrins and derivatives as well as for transition metal complexes. The calculations were performed taking into account the solvation effects. Solvation was included by solving the Poisson-Boltzmann equations with a realistic molecular surface (van der Waals radius plus solvent radius about each atom) using the Jaguar solvation model (PBF) [41]. We used a dielectric constant of 80.37 and a probe radius of 1.4 Å for water. The properties established were ESP charges. These results are considered for docking calculation performed by Glide (see next paragraph).

4.5.3. Molecular docking

Molecular Docking was carried out by Glide software [42] using the ligands and the Fe(II)-heme prepared as above-mentioned, applying Glide extra precision (SP) method. The charges calculated and derived from the QM calculation were considered for docking calculations by applying the OPLS_2005 force field. The grid was generated considering the iron atom as the center of it and restricting it to the length of the ligands used in the present study in order to establish its size. The compounds were docked with default parameters, with the constraint of a metal charged acceptor. The number of poses entered to post-docking minimization was set to 10. Glide SP score was then evaluated. A single best conformation of each ligand was considered for the further evaluation of the binding energy.

4.5.4. Prime/MM-GBSA simulation

The Prime/MM-GBSA method implemented in Prime software [43] consists in computing the change between the free and the complex state of both the ligand and the heme after energy minimization. The technique was applied using the docking complexes obtained in the docking protocol. The software was used to calculate the free-binding energy (ΔG_{bind}) of each ligand, as recently reported by us [44–47].

Acknowledgments

Financial contribution from MIUR is kindly acknowledged (Project PRIN 20154JRJPP).

Appendix A. Supplementary material

Supplementary data to this article can be found online at https://doi.org/10.1016/j.bioorg.2019.103020.

References

[1] World Malaria Report 2018. (04/03/2019).
[2] C. Amaratunga, P. Lim, S. Suon, S. Sreng, S. Mao, C. Sopha, B. Sam, D. Dek, V. Try, R. Amato, D. Blessborn, L. Song, G.S. Tullo, M.P. Fay, J.M. Anderson, J. Tarning, R.M. Fairhurst, Dihydroartemisinin-piperaquine resistance in Plasmodium falciparum malaria in Cambodia: a multisite prospective cohort study, Lancet Infect. Dis. 16 (2016) 357–365.
[3] F. Ariey, B. Witkowski, C. Amaratunga, J. Beghain, A.C. Langlois, N. Khim, S. Kim, V. Duru, C. Bouchier, L. Ma, P. Lim, R. Leang, S. Duong, S. Sreng, S. Suon, C.M. Chuor, D.M. Bout, S. Menard, W.O. Rogers, B. Genton, et al., A molecular marker of artemisinin-resistant Plasmodium falciparum malaria, Nature 505 (2014) 50–55.
[4] R. Hooft van Huijsduijnen, T.N. Wells, The antimalarial pipeline, Curr. Opin. Pharmacol. 42 (2018) 1–6.
[5] S.F. Mossallam, E.I. Amer, M.H. El-Faham, Efficacy of Synriam, a new antimalarial combination of OZ277 and piperaquine, against different developmental stages of Schistosoma mansoni, Acta Trop. 143 (2015) 36–46.
[6] P.M. O'Neill, R.K. Amewu, S.A. Charman, S. Sabbani, N.F. Gnadig, J. Straimer, D.A. Fidock, E.R. Shore, N.L. Roberts, M.H. Wong, W.D. Hong, C. Pidathala, C. Riley, B. Murphy, G. Aljayyoussi, F.J. Gamo, L. Sanz, J. Rodrigues, C.G. Cortes, E. Herreros, et al., A tetraoxane-based antimalarial drug candidate that overcomes PfK13-C580Y dependent artemisinin resistance, Nat. Commun. 8 (2017) 15159.
[7] F. Baumgaertner, J. Jourdan, C. Scheurer, B. Blasco, B. Campo, P. Maeser, S. Wittlin, In vitro activity of anti-malarial ozonides against an artemisinin-resistant isolate, Malar. J. 16 (2017) 45/41-45/46.
[8] J. Straimer, N.F. Gnadig, B.H. Stokes, M. Ehrenberger, A.A. Crane, D.A. Fidock, Plasmodium falciparum K13 mutations differentially impact ozonide susceptibility and parasite fitness in vitro, MBio 8 (2017).
[9] H.M. Ismail, V.E. Barton, M. Panchana, S. Charoensutthivarakul, G.A. Biagini, S.A. Ward, P.M. O'Neill, A click chemistry-based proteomic approach reveals that 1,2,4-trioxolane and artemisinin antimalarials share a common protein alkylation profile, Angew. Chem. Int. Ed. Engl. 55 (2016) 6401–6405.
[10] J. Wang, C.J. Zhang, W.N. Chia, C.C.Y. Loh, Z.J. Li, Y.M. Lee, Y.K. He, L.X. Yuan, T.K. Lim, M. Liu, C.X. Liew, Y.Q. Lee, J.B. Zhang, N.C. Lu, C.T. Lim, Z.C. Hua, B. Liu, H.M. Shen, K.S.W. Tan, Q.S. Lin, Haem-activated promiscuous targeting of artemisinin in Plasmodium falciparum, Nature Commun. (2015) 6.
[11] G.H. Posner, C.H. Oh, A Regiospecifically O-18 labeled 1,2,4-trioxane - a simple chemical-model system to probe the mechanism(S) for the antimalarial activity of artemisinin (Qinghaosu), J. Am. Chem. Soc. 114 (1992) 8328–8329.
[12] W.M. Wu, Y.K. Wu, Y.L. Wu, Z.J. Yao, C.M. Zhou, Y. Li, F. Shan, Unified mechanistic framework for the Fe(II)-induced cleavage of Qinghaosu and derivatives/analogues. The first spin-trapping evidence for the previously postulated secondary C-4 radical (vol 120, pg 3316, 1998), J. Am. Chem. Soc. 120 (1998) 13002.
[13] P.L. Olliaro, R.K. Haynes, B. Meunier, Y. Yuthavong, Possible modes of action of the artemisinin-type compounds, Trends Parasitol. 17 (2001) 122–126.
[14] Y. Wu, Z.Y. Yue, Y.L. Wu, Interaction of Qinghaosu (Artemisinin) with cysteine sulfhydryl mediated by traces of non-heme iron, Angew. Chem. Int. Ed. Engl. 38 (1999) 2580–2582.
[15] Y. Wu, How might qinghaosu (artemisinin) and related compounds kill the intraerythrocytic malaria parasite? A chemist's view, Acc. Chem. Res. 35 (2002) 255–259.
[16] S.R. Meshnick, The mode of action of antimalarial endoperoxides, Trans R. Soc. Trop. Med. Hyg. 88 (Suppl 1) (1994) S31–S32.
[17] S. Krishna, A.C. Uhlemann, R.K. Haynes, Artemisinins: mechanisms of action and potential for resistance, Drug Resist. Updat. 7 (2004) 233–244.
[18] R.K. Haynes, K.W. Cheu, H.W. Chan, H.N. Wong, K.Y. Li, M.M. Tang, M.J. Chen, Z.F. Guo, Z.H. Guo, K. Sinniah, A.B. Witte, P. Coghi, D. Monti, Interactions between artemisinins and other antimalarial drugs in relation to the cofactor model–a unifying proposal for drug action, ChemMedChem 7 (2012) 2204–2226.
[19] R.K. Haynes, K.W. Cheu, M.M. Tang, M.J. Chen, Z.F. Guo, Z.H. Guo, P. Coghi, D. Monti, Reactions of antimalarial peroxides with each of leucomethylene blue and

dihydroflavins: flavin reductase and the cofactor model exemplified, ChemMedChem 6 (2011) 279–291.
[20] S. Gemma, E. Gabellieri, S. Sanna Coccone, F. Marti, O. Taglialatela-Scafati, E. Novellino, G. Campiani, S. Butini, Synthesis of dihydroplakortin, 6-epi-dihydroplakortin, and their C10-desethyl analogues, J. Org. Chem. 75 (2010) 2333–2340.
[21] S. Gemma, F. Marti, E. Gabellieri, G. Campiani, E. Novellino, S. Butini, Synthetic studies toward 1,2-dioxanes as precursors of potential endoperoxide-containing antimalarials, Tetrahedron Lett. 50 (2009) 5719–5722.
[22] S. Gemma, S. Kunjir, S.S. Coccone, M. Brindisi, V. Moretti, S. Brogi, E. Novellino, N. Basilico, S. Parapini, D. Taramelli, G. Campiani, S. Butini, Synthesis and antiplasmodial activity of bicyclic dioxanes as simplified dihydroplakortin analogues, J. Med. Chem. 54 (2011) 5949–5953.
[23] S. Gemma, S. Kunjir, M. Brindisi, E. Novellino, G. Campiani, S. Butini, A synthetic strategy to bridged 2,3,8-trioxabicyclo[3,3,1]nonane endoperoxides, Tetrahedron Lett. 54 (2013) 1233–1235.
[24] M. Brindisi, S. Gemma, S. Kunjir, L. Di Cerbo, S. Brogi, S. Parapini, S. D'Alessandro, D. Taramelli, A. Habluetzel, S. Tapanelli, S. Lamponi, E. Novellino, G. Campiani, S. Butini, Synthetic spirocyclic endoperoxides: new antimalarial scaffolds, Medchemcomm 6 (2015) 357–362.
[25] O. Taglialatela-Scafati, E. Fattorusso, A. Romano, F. Scala, V. Barone, P. Cimino, E. Stendardo, B. Catalanotti, M. Persico, C. Fattorusso, Insight into the mechanism of action of plakortins, simple 1,2-dioxane antimalarials, Org. Biomol. Chem. 8 (2010) 846–856.
[26] P.M. O'Neill, S. Hindley, M.D. Pugh, J. Davies, P.G. Bray, B.K. Park, D.S. Kapu, S.A. Ward, P.A. Stocks, Co(thd)(2): a superior catalyst for aerobic epoxidation and hydroperoxysilylation of unactivated alkenes: application to the synthesis of spiro-1,2,4-trioxanes, Tetrahedron Lett. 44 (2003) 8135–8138.
[27] A. Vallone, S. D'Alessandro, S. Brogi, M. Brindisi, G. Chemi, G. Alfano, S. Lamponi, S.G. Lee, J.M. Jez, K.J.M. Koolen, K.J. Dechering, S. Saponara, F. Fusi, B. Gorelli, D. Taramelli, S. Parapini, R. Caldelari, G. Campiani, S. Gemma, S. Butini, Antimalarial agents against both sexual and asexual parasites stages: structure-activity relationships and biological studies of the Malaria Box compound 1-[5-(4-bromo-2-chlorophenyl)furan-2-yl]-N-[(piperidin-4-yl)methyl]methanamine (MMV019918) and analogues, Eur. J. Med. Chem. 150 (2018) 698–718.
[28] F. Bousejra-El Garah, M.H. Wong, R.K. Amewu, S. Muangnoicharoen, J.L. Maggs, J.L. Stigliani, B.K. Park, J. Chadwick, S.A. Ward, P.M. O'Neill, Comparison of the reactivity of antimalarial 1,2,4,5-tetraoxanes with 1,2,4-trioxolanes in the presence of ferrous iron salts, heme, and ferrous iron salts/phosphatidylcholine, J. Med. Chem. 54 (2011) 6443–6455.
[29] A.M. Szpilman, E.E. Korshin, R. Hoos, G.H. Posner, M.D. Bachi, Iron(II)-induced degradation of antimalarial beta-sulfonyl endoperoxides. Evidence for the generation of potentially cytotoxic carbocations, J. Org. Chem. 66 (2001) 6531–6540.
[30] P.M. O'Neill, L.P.D. Bishop, N.L. Searle, J.L. Maggs, R.C. Storr, S.A. Ward, B.K. Park, Mabbs F. Biomimetic Fe(II)-mediated degradation of arteflene (Ro-42-1611). The first EPR spin-trapping evidence for the previously postulated secondary carbon-centered cyclohexyl radical, J. Org. Chem. 65 (2000) 1578–1582.
[31] A. Alberti, D. Macciantelli, Spin trapping, in: M. Brustolon, E. Giamello (Eds.), Electron Paramagnetic Resonance, Wiley, 2008Chapter 8.
[32] Y. Tang, Y. Dong, X. Wang, K. Sriraghavan, J.K. Wood, J.L. Vennerstrom, Dispiro-1,2,4-trioxane analogues of a prototype dispiro-1,2,4-trioxolane: mechanistic comparators for artemisinin in the context of reaction pathways with iron(II), J. Org. Chem. 70 (2005) 5103–5110.
[33] X. Wang, Y. Dong, S. Wittlin, D. Creek, J. Chollet, S.A. Charman, J.S. Tomas, C. Scheurer, C. Snyder, J.L. Vennerstrom, Spiro- and dispiro-1,2-dioxolanes: contribution of iron(II)-mediated one-electron vs two-electron reduction to the activity of antimalarial peroxides, J. Med. Chem. 50 (2007) 5840–5847.
[34] W. Trager, J.B. Jensen, Human malaria parasites in continuous culture, Science 193 (1976) 673–675.
[35] S. Gemma, C. Camodeca, S. Sanna Coccone, B.P. Joshi, M. Bernetti, V. Moretti, S. Brogi, M.C. Bonache de Marcos, L. Savini, D. Taramelli, N. Basilico, S. Parapini, M. Rottmann, R. Brun, S. Lamponi, S. Caccia, G. Guiso, R.L. Summers, R.E. Martin, S. Saponara, et al., Optimization of 4-aminoquinoline/clotrimazole-based hybrid antimalarials: further structure-activity relationships, in vivo studies, and preliminary toxicity profiling, J. Med. Chem. 55 (2012) 6948–6967.
[36] M.T. Makler, J.M. Ries, J.A. Williams, J.E. Bancroft, R.C. Piper, B.L. Gibbins, D.J. Hinrichs, Parasite lactate dehydrogenase as an assay for Plasmodium falciparum drug sensitivity, Am. J. Trop. Med. Hyg. 48 (1993) 739–741.
[37] International Standards Organization. Biological evaluation of medical devices—Part 5: tests for cytotoxicity: in vitro methods. (2009-06) [2018-08-01]. < https://www.iso.org/standard/36406.html > .
[38] LigPrep. version 3.5, Schrödinger, LLC, New York, NY, 2015.
[39] MacroModel. version 10.9, Schrödinger, LLC, New York, NY, 2015.
[40] Jaguar, version 8.9, Schrödinger, LLC, New York, NY, 2015.
[41] D.J. Tannor, B. Marten, R. Murphy, R.A. Friesner, D. Sitkoff, A. Nicholls, M. Ringnalda, W.A. Goddard, B. Honig, Accurate first principles calculation of molecular charge-distributions and solvation energies from ab-initio quantum-mechanics and continuum dielectric theory, J. Am. Chem. Soc. 116 (1994) 11875–11882.
[42] Glide, version 6.8, Schrödinger, LLC, New York, NY, 2015.
[43] Prime. version 4.1, Schrödinger, LLC, New York, NY, 2015.
[44] S. Brogi, A. Fiorillo, G. Chemi, S. Butini, M. Lalle, A. Ilari, S. Gemma, G. Campiani, Structural characterization of Giardia duodenalis thioredoxin reductase (gTrxR) and computational analysis of its interaction with NBDHEX, Eur. J. Med. Chem. 135 (2017) 479–490.
[45] S. Giovani, M. Penzo, S. Butini, M. Brindisi, S. Gemma, E. Novellino, G. Campiani, M.J. Blackman, S. Brogi, Plasmodium falciparum subtilisin-like protease 1: discovery of potent difluorostatone-based inhibitors, RSC Adv. 5 (2015) 22431–22448.
[46] M. Paolino, M. Brindisi, A. Vallone, S. Butini, G. Campiani, C. Nannicini, G. Giuliani, M. Anzini, S. Lamponi, G. Giorgi, D. Sbardella, D.M. Ferraris, S. Marini, M. Coletta, I. Palucci, M. Minerva, G. Delogu, I. Pepponi, D. Goletti, A. Cappelli, et al., Development of potent inhibitors of the mycobacterium tuberculosis virulence factor zmp1 and evaluation of their effect on mycobacterial survival inside macrophages, Chemmedchem 13 (2018) 422–430.
[47] M. Brindisi, S. Maramai, S. Gemma, S. Brogi, A. Grillo, L.D. Mannelli, E. Gabellieri, S. Lamponi, S. Saponara, B. Gorelli, D. Tedesco, T. Bonfiglio, C. Landry, K.M. Jung, A. Armirotti, L. Luongo, A. Ligresti, F. Piscitelli, C. Bertucci, M.P. Dehouck, et al., Development and pharmacological characterization of selective blockers of 2-arachidonoyl glycerol degradation with efficacy in rodent models of multiple sclerosis and pain, J. Med. Chem. 59 (2016) 2612–2632.